

Topical Review

Theoretical tools for the description of charge transport in disordered organic semiconductors

A V Nenashev^{1,2}, J O Oelerich³ and S D Baranovskii³

¹ Institute of Semiconductor Physics, 630090 Novosibirsk, Russia

² Novosibirsk State University, 630090 Novosibirsk, Russia

³ Faculty of Physics and Material Sciences Center, Philipps-Universität, D-35032 Marburg, Germany

E-mail: baranovs@staff.uni-marburg.de

Received 1 October 2014, revised 28 October 2014

Accepted for publication 7 January 2015

Published 11 February 2015



CrossMark

Abstract

Hopping conduction is widely considered the dominant charge transport mechanism in disordered organic semiconductors. Although theories of hopping transport have been developed in detail for applications to inorganic amorphous materials, these theories are often out of scope for the community working with organic amorphous systems. Theoretical research on charge transport in organic systems is overwhelmed by phenomenological fittings of numerical results by equations, which often make little physical sense. The aim of the current review is to bring analytical theoretical methods to the attention of the community working with disordered organic semiconductors.

Keywords: charge transport, disorder, organic semiconductors

(Some figures may appear in colour only in the online journal)

1. Introduction

Electronic properties of organic disordered semiconductors (ODSs) are currently the focus of intensive experimental and theoretical research. ODSs already dominate the industrial electrophotographic image recording and their applications in light-emitting diodes (OLEDs) [1, 2], in field-effect transistors (OFETs) [3] and in organic solar cells (OSCs) [4] are intensively worked on. ODSs are a broad class of materials, which can essentially differ from each other in morphology and chemical composition. Most prominent representatives of the ODSs are conjugated polymers [5, 6], molecularly doped polymers [7–9] and low-molecular-weight organic glasses [10, 11]. Understanding the electronic properties of the ODSs is challenging with respect to the fundamental research and device development. In the current report, we focus on the theoretical tools suitable for description of charge transport properties of the ODSs, bearing in mind that charge transport is decisive for all device applications of such materials.

In spite of the broad variety in the materials' chemistry and morphology, it is widely accepted that charge transport in most ODSs is due to incoherent tunneling (hopping) of electrons or holes between strongly localized states, which are distributed randomly in space. This was shown by Bäessler in two detailed review papers [9, 12] and confirmed later in numerous review articles, monographs and edited books about charge transport in ODSs [13–24]. The frequency of a hopping transition from an occupied site i to an empty site j is typically [9, 12, 24] described either by the Miller–Abrahams (MA) expression [25]

$$v_{ij} = v_0 \exp\left(-\frac{2r_{ij}}{\alpha} - \frac{\varepsilon_j - \varepsilon_i + |\varepsilon_i - \varepsilon_j|}{2kT}\right), \quad (1)$$

or [26] by the Marcus expression [27]

$$v_{ij} = \frac{J_o^2}{\hbar} \sqrt{\frac{\pi}{4E_a kT}} \exp\left(-\frac{2r_{ij}}{\alpha} - \frac{E_a}{kT}\right) \times \exp\left(-\frac{\varepsilon_j - \varepsilon_i}{2kT} - \frac{(\varepsilon_j - \varepsilon_i)^2}{16kT E_a}\right). \quad (2)$$

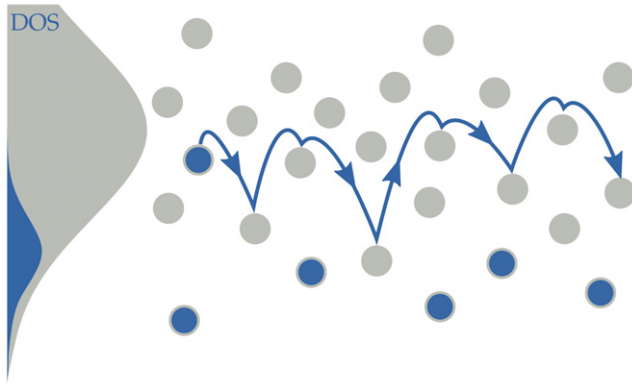


Figure 1. Charge carrier motion via hopping in the Gaussian DOS. Occupied states are marked blue.

In equations (1) and (2), α is the localization length of charge carriers in the localized states, which takes values of the order of 10^{-8} cm [7, 28], ε_i and ε_j are the energies of the states i and j , respectively, k is the Boltzmann constant and T is temperature. The prefactor ν_0 in equation (1) depends on the interaction mechanism responsible for the hopping transitions and is called the *attempt-to-escape frequency*. Usually, electron-phonon interaction is assumed, with ν_0 being close to the phonon frequency 10^{12} s $^{-1}$ [12, 29]. The prefactor J_o^2 in equation (2) is related to the transfer integral connecting the sites involved in the transition and E_a is the polaron activation energy related to the reorganization energy of the matrix.

Often, a Gaussian density of states (DOS) is assumed for organic disordered materials [9, 12],

$$g(\varepsilon) = \frac{N}{\sigma\sqrt{2\pi}} \exp\left(-\frac{\varepsilon^2}{2\sigma^2}\right). \quad (3)$$

In equation (3), σ is the characteristic energy scale of the disorder, which in ODSs is usually of the order of $\sigma \approx 0.1$ eV [9] and N is the concentration of localized states, typically between $N \simeq 10^{20}$ cm $^{-3}$ and $N \simeq 10^{21}$ cm $^{-3}$ [30–37]. It was recently proven that the organic semiconductors P3HT, OC $_1$ C $_{10}$ -PPV and quinquethiophenes (5T) possess a Gaussian DOS [24, 38], confirming the claim of BäSSLER [9, 12]. The corresponding model is called the *Gaussian Disorder Model* (GDM) when spatial positions and energies can be considered as independent from each other. If, in the opposite case, site positions and energies are correlated, one usually speaks of the *Correlated Disorder Model* (CDM) [39, 40]. The DOS in the CDM can be Gaussian as well. Hopping motion in the Gaussian DOS is schematically shown in figure 1.

Sometimes a purely exponential DOS is assumed in the literature [32, 41–59]:

$$g(\varepsilon) = \frac{N}{\varepsilon_0} \exp\left(\frac{\varepsilon}{\varepsilon_0}\right). \quad (4)$$

We denote the energy scale in equation (4) as ε_0 in order to distinguish it in the following discussion from the energy scale σ of the Gaussian DOS given by equation (3).

In spite of the clearly formulated model, the development of theoretical research related to charge transport in ODSs

cannot be considered satisfactory. It is particularly unsatisfactory when we take into account the fact that comprehensive theories for the description of hopping transport in inorganic disordered systems, such as doped crystalline and amorphous inorganic semiconductors, have existed for decades and been successfully applied to the description of similar processes. Most prominent representatives of the latter systems are chalcogenide glasses, like amorphous selenium (a-Se) and amorphous semiconductors, like hydrogenated amorphous silicon (a-Si:H). The DOS function in such materials is believed to be purely exponential, as given by equation (4) [19]. The theory of hopping charge transport in the exponential DOS was developed in detail in the 1970s. This theory is, however, only rarely applied to ODSs. Most researchers working with ODSs are instead focused on equations obtained by phenomenological fitting of numerical results. Two almost non-overlapping worlds seem to coexist: The world of theory (WoT), in which researchers use well approved analytical methods developed to describe hopping transport and the world of simulations (WoS), in which computers are made responsible for developing analytical equations on the basis of numerical simulations. The aim of the current report is to discuss the state of affairs in the WoS and WoT and to highlight theoretical tools appropriate for the treatment of ODSs in the WoT.

It will be shown in section 2 that equations provided in the WoS by phenomenological fitting of numerical results, albeit very popular, can seldomly be considered as reliable. In the succeeding sections, analytical theories to describe hopping transport in application to ODSs will be discussed. This report is complementary to the recently published review articles by Tessler *et al* [22] and by Baranovskii [24]. The paper by Tessler *et al* [22] focused mainly on applications of general transport concepts to organic thin-film devices, while the review by Baranovskii [24] focused on the applications of the general theoretical concepts to account for particular dependences of the carrier mobility on the concentration of charge carriers, on temperature, on the applied electric field, on the concentration of hopping sites etc, without going into detail on the analytical theories. In the current report, we pay much attention to the details of the theoretical concepts, so that one could use the text as a guide for calculations. In particular, the *percolation theory* and the concept of the *transport energy* and their application to the *variable-range hopping* (VRH) problem are highlighted in detail. In addition, a new analytical approach to VRH based on calculations of the dissipated heat in a resistor network is described.

2. WoS: phenomenological fitting of numerical results

As indicated in the introduction, there exists a broad community of researchers who numerically simulate transport properties in ODSs for some given sets of parameters and appoint a computer to provide analytical equations suitable to describe the numerical data. The corresponding equations mostly lack any theoretical or physical basis. We shall call this community the *World of Simulations* (WoS). Let us highlight the dangers of the phenomenological fitting in the case of the

two most popular equations in the field of ODSs obtained in the framework of the GDM.

In the seminal review article by Bäessler [9], the dependence of the carrier mobility μ on the strength of electric field F in the GDM with MA rates was given in the form

$$\mu(F) = \mu_0 \exp \left\{ - \left(\frac{2}{3} \frac{\sigma}{kT} \right)^2 \right\} \times \exp \left\{ \tilde{C} \left[\left(\frac{\sigma}{kT} \right)^2 - \tilde{B} \right] \sqrt{F} \right\}. \quad (5)$$

Here μ_0 is a field-independent prefactor and $\tilde{B} = 2.25$ for $\Sigma < 1.5$ and $\tilde{B} = \Sigma^2$ for $\Sigma \geq 1.5$, with Σ being the numerical parameter of the so-called *non-diagonal disorder* responsible for the variation of the intersite coupling on a lattice [9]. For a spatially random distribution of sites, this extra parameter Σ would correspond to the additional random distribution of localization parameters α . This equation has been noted as the most widely used equation in the context of organic semiconductors [22]. Usually, experimentally measured dependences $\mu(F)$ are compared to equation (5) in an attempt to determine material parameters [60–62].

A rather similar approach to determine $\mu(F)$ was used by Pasveer *et al* [33], who also numerically determined $\mu(F)$ in the GDM with MA rates on a lattice and fitted the results by the analytical formula

$$\mu(T, n, F) \approx \mu(T, n) \phi(T, F), \quad (6)$$

with $\phi(T, F)$ in the form:

$$\phi(T, F) = \exp \left\{ 0.44 \left[\left(\frac{\sigma}{kT} \right)^{3/2} - 2.2 \right] \times \left[\sqrt{1 + 0.8 \left(\frac{Feb}{\sigma} \right)^2} - 1 \right] \right\}, \quad (7)$$

where b is the lattice constant.

It is remarkable that equations (5)–(7) are very popular in the field of ODSs in spite of the fact that these equations can hardly be correct. At small energy disorder, $\sigma < 1.5kT$, for equation (5) and $\sigma < 1.7kT$, for equation (7), when the exponents in these equations become negative, both equations predict exponential decrease of the carrier mobility with rising electric field at all field values. This result can hardly be rationalized if we take into account that the increase of the mobility at low fields was predicted in numerous transparent theoretical calculations of hopping conductivity [63–65].

In the opposite case of high energy disorder, $\sigma > 1.5kT$ for equation (5) and $\sigma > 1.7kT$ for equation (7), when the exponents become positive, both equations predict exponential increase of the mobility with rising electric field at any field. Let us consider equation (7) and show that this equation is erroneous at high electric fields. At $eFb > \sigma$ we can assume $\sqrt{1 + 0.8(eFb/\sigma)^2} \propto F$ and $\phi(T, F)$ of equation (6) therefore becomes exponentially increasing as a function of the field strength F . One should note, however, that if the inequality $Feb > \sigma$ is valid, the energy gain of a charge carrier due

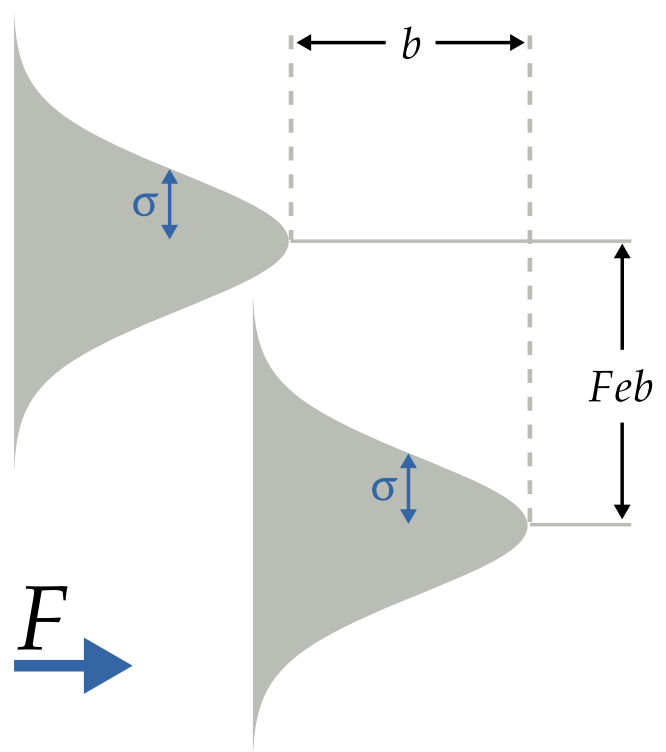


Figure 2. By hopping over a distance b along the field direction, the (positively charged) carrier gains energy Feb , which is to be compared with the energy scale of disorder σ .

to hopping transitions over the shortest possible distance b along the field direction is larger than the energy scale σ of the DOS, as illustrated in figure 2. Under these circumstances, disorder does not provide any obstacle for hopping motion with MA rates and the drift velocity v_d is field-independent. Concomitantly, the drift mobility $\mu = v_d/F$ should decrease with rising field as $\mu \propto 1/F$ at $Feb > \sigma$. This clearly conflicts with the prediction of equation (7). Apparently, equation (7) cannot be valid at $\sigma > 1.7kT$ and $Feb > \sigma$. Notably, this invalidity is not only quantitative but also qualitative: While equation (7) predicts an exponential increase of μ with rising F , in reality μ decreases with F . The same deficiency can also be found in equation (5).

The lack of awareness of the WoS with respect to the main results obtained in the WoT for description of hopping conduction is striking. For instance, simulating the carrier mobility at different carrier concentrations n in the framework of the GDM in 2005, Pasveer *et al* [33] recognized a concentration dependence of the mobility $\mu(n)$. Although the dependence of the mobility μ on carrier concentration n in the hopping regime is a trivial effect, well-known to the scientific community for decades, it somehow appeared remarkable for researchers working with ODSs [33, 43, 46] and the GDM was renamed as the *Extended Gaussian Disorder Model* (EGDM) [66].

Let us therefore briefly reason why the hopping mobility should be inherently concentration-dependent. The transition rates of a charge carrier hopping between a pair of sites i and j given in equation (1) are valid only if site i is occupied by a charge carrier and site j is empty. In the general case, the

contribution of the pair of sites i and j to charge transport depends on the position of the Fermi level ε_F [25]:

$$v_{ij} = v_0 \exp\left(-\frac{2r_{ij}}{\alpha} - \frac{|\varepsilon_i - \varepsilon_j| + |\varepsilon_i - \varepsilon_F| + |\varepsilon_j - \varepsilon_F|}{2kT}\right). \quad (8)$$

As a consequence of equation (8), pairs of sites i and j play little role for charge transport when both sites are likely to be unoccupied, i.e. energies ε_i and ε_j lie far above ε_F , or both sites are blocked by charge carriers when the energies ε_i and ε_j are far below ε_F . Since the transition rates therefore depend decisively on the carrier concentration n via $\varepsilon_F(n)$, the carrier mobility μ should depend on n as well. In many experimental studies of ODSs, however, the dependence $\mu(n)$ is *not* observed at low n , which is a remarkable and unexpected result. The issue of the concentration-independent mobility is discussed in section 3.3.

With respect to ODSs, the dependence of μ on n has been recognized as an inherent property of Bässler's GDM in numerous theoretical studies [31, 67–72]. For instance, Shaked *et al* [71] clearly stated '*that within the disorder-model framework developed by Bässler and co-workers [14] it is possible to account for strong density dependence of the mobility*'. Furthermore, Schmechel [69, 70] demonstrated the ability of the GDM to provide the concentration-dependent mobilities in ODSs and applied his analysis to account for existing experimental data. Apparently being unaware of this development achieved in the WoT, researchers in the WoS promoted their numerical result as the new EGDM [33, 66].

The above analysis of equations (5)–(7), which belong to the most cited of theoretical results in the field of ODSs, shows that acting in the framework of the WoS can hardly lead to rational conclusions and that naively following its results can be dangerous. Empirical fitting of numerical data not supported by solid theoretical concepts can be valid in some restricted range of parameters, but not in general. Some dependences of transport coefficients on material parameters were considered in the WoS as universal simply because other parameters were not changed in course of simulations. Therefore we dedicate the rest of this report to theoretical concepts developed in the WoT for description of charge transport in the hopping regime.

Application of equations (6) and (7) can have another, not just academic, consequence. As announced in the recent feature article by Coehoorn and Bobbert [66], such phenomenological equations are the basis for the commercially available OLED simulation software tools (Simulation software SETFOS3.2, product of Fluxim (www.fluxim.com); Simulation software SimOLED3.x, product of Sim4tec (www.sim4tec.com)). The accuracy of the commercially available software is, however, out of the scope of our report.

3. WoT: general remarks on transport regimes

Before diving into details of the analytical tools developed to study hopping charge transport in disordered materials, let us first discuss some characteristic regimes of the long-range hopping transport and address the decisive properties of the

energy spectrum of the ODSs. In particular, we will discuss in the following sections when hopping transport can be treated as nearest-neighbour hopping (NNH) and when the more general regime of the variable-range hopping (VRH) should be considered. Furthermore, under which circumstances one can model charge transport on regular lattice grids and what influence the shape of the DOS has on the transport properties, will be discussed.

3.1. Nearest-neighbour or variable-range hopping?

Due to the dependences of the hopping rates given by equations (1) and (2) on the intersite distances r_{ij} and on site energies ε_i , ε_j , hopping conduction is in general a variable-range hopping (VRH) process. At low temperatures, as compared to the energy scale of disorder, energy factors in the exponents of equations (1) and (2) play an essential role and carriers mostly tunnel to spatially remote sites in order to optimize the activation in energy. The higher T is, the less important the energy-dependent factors become and the closer in space the carrier transitions are, as prescribed by the tunneling probability $\exp(-2r_{ij}/\alpha)$ in equations (1) and (2). In the limit of sufficiently high temperatures, when $kT > \sigma$ in equation (3) or $kT > \varepsilon_0$ in equation (4), only spatial factors determine the hopping rates and the VRH regime turns into the nearest-neighbour hopping (NNH) regime, in which carriers mostly tunnel to the spatially nearest sites [73].

Sometimes it is argued that the VRH cannot serve as the appropriate transport mechanism in ODSs consisting of large molecules, as illustrated in figure 3(a). At first glance, it seems that only the NNH is possible in such media, because the nearest neighbours block the electron's way to more distant molecules, preventing the long-distance jumps. If so, the localization sites are often placed on a regular lattice grid and it is assumed that hopping transitions are possible only between the nearest neighbours even at low temperatures, $kT \ll \sigma$ [74, 75].

Below, we show that these naive arguments against the VRH are irrelevant. The nearest neighbours do not block distant jumps. Indeed, they even enhance the probability of such jumps due to the broader spread of the electron wavefunctions. As a result of such spreading, the effective localization length in a dense array of molecules turns out to be larger than that in a single-molecule case.

Let us prove this effect for the simplest model: the one-dimensional model of Anderson localization with equally spaced potential wells, whose energy levels are randomly distributed (figure 3(b)). Let D be the distance between the centers of the wells, σ —the characteristic scatter of the energy levels and τ —the hopping integral (tunneling integral) between the adjacent wells. We consider only the case of a strong Anderson localization, where $\tau \ll \sigma$. Wells are numbered from left to right, so that the coordinate of the n th well is $x_n = Dn$.

According to the tight-binding approach, the electron wavefunction is characterized by the set $\{\dots, a_{-1}, a_0, a_1, a_2, \dots\}$ of amplitudes (expansion coefficients) related to the corresponding wells (figure 3(c)). Let us consider the localized

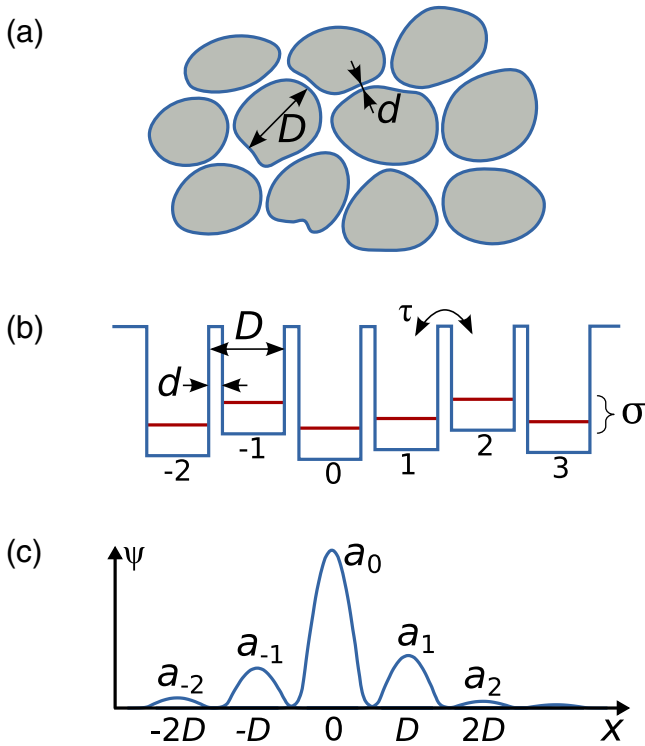


Figure 3. Dense array of organic molecules: (a) schematic representation; the molecule diameter D is large compared with the intermolecular distance d ; (b) one-dimensional model of potential wells with energy disorder (Anderson model); (c) typical shape of the electron wavefunction in a strongly localized state; amplitudes a_n are related to probabilities p_n of finding the electron in corresponding wells as $|a_n|^2 = p_n$.

state centered at the 0th well, so that the amplitude a_0 is the largest one. It is easy to see (e.g., from the first-order perturbation theory) that

$$a_{\pm 1} \approx a_0 \frac{\tau}{\Delta \varepsilon_{0,\pm 1}}, \quad (9)$$

where $\Delta \varepsilon_{mn}$ is the energy difference between the m th and the n th sites [73]. The typical values of this difference are of the order of σ and therefore

$$\frac{|a_{\pm 1}|}{|a_0|} \approx \frac{\tau}{\sigma}. \quad (10)$$

Analogous consideration shows that this estimate holds also for more distant wells:

$$\frac{|a_{\pm(n+1)}|}{|a_{\pm n}|} \approx \frac{\tau}{\sigma} \quad \text{for } n \geq 0. \quad (11)$$

Applying equation (11) repeatedly, one can see that

$$|a_n| \approx |a_0| \left(\frac{\tau}{\sigma} \right)^{|n|}, \quad (12)$$

i.e. amplitudes a_n decay exponentially with distance from the central (0th) well. This decay can be expressed as

$$|a_n| \approx |a_0| \exp\left(-\frac{|x_n|}{\alpha_{\text{eff}}}\right), \quad (13)$$

where $x_n = Dn$ is the position of the n th well (with respect to the well at which the wavefunction is centered) and α_{eff} is the effective localization radius. The value of α_{eff} can be obtained by comparison between equations (12) and (13):

$$\alpha_{\text{eff}} = \frac{D}{\ln(\sigma/\tau)}. \quad (14)$$

Now let us return to the dense three-dimensional array of large molecules. One can expect that equation (14) is valid in this case at least qualitatively, since there is nothing special to the one-dimensional Anderson model in the considerations above. (In the three-dimensional case, one should consider D as the diameter of the molecules.) One can conclude from equation (14) that α_{eff} and D have the same order of magnitude (unless τ is smaller than σ by many orders of magnitude), which makes variable-range hopping possible. In a localized state, the wavefunction penetrates not only into the adjacent molecules, but also into the more remote ones. Therefore, hops between the non-nearest-neighbouring molecules contribute to the hopping transport.

Let us express the effective localization length α_{eff} via the bare localization length in the barrier, α_0 . It is obvious that the tunneling integral τ depends on the barrier thickness d as $\propto \exp(-d/\alpha_0)$. The preexponential factor can be roughly estimated quasiclassically [76, section 50], yielding

$$\tau \approx \frac{\Delta E}{2\pi} \exp\left(-\frac{d}{\alpha_0}\right), \quad (15)$$

where ΔE is the typical distance between the energy levels in a single molecule. Substituting equation (15) into equation (14), one obtains the relation between the bare and the ‘effective’ localization radii, α_0 and α_{eff} :

$$\alpha_{\text{eff}} \approx \frac{D}{d/\alpha_0 - \ln(\Delta E/2\pi\sigma)}. \quad (16)$$

Here, both d (spacing between the molecules) and α_0 are of the order of several Ångströms, hence d/α_0 is not a large number. The same is true for $\ln(\Delta E/2\pi\sigma)$. Therefore, one can see again, that α_{eff} has the order of D (molecule diameter), rather than of α_0 .

The arguments above can be viewed as a justification of the dominating role of the VRH in organic semiconductors, both for small and large molecules as compared to the intermolecular distance. It is therefore important to account for the VRH regime when dealing with ODSs in theoretical studies.

3.2. When are lattice models appropriate?

Very often, studies of charge transport, particularly in the WoS, are performed on regular lattice grids, although the characteristic property of disordered materials is not only the energetic, but also the *spatial* disorder. Such studies can well mimic the VRH regime as long as the decisive temperature-dependent length of the hops in the VRH essentially exceeds the lattice constant of the grid and hops to remote lattice sites are included [9]. However, studies on grids make little sense

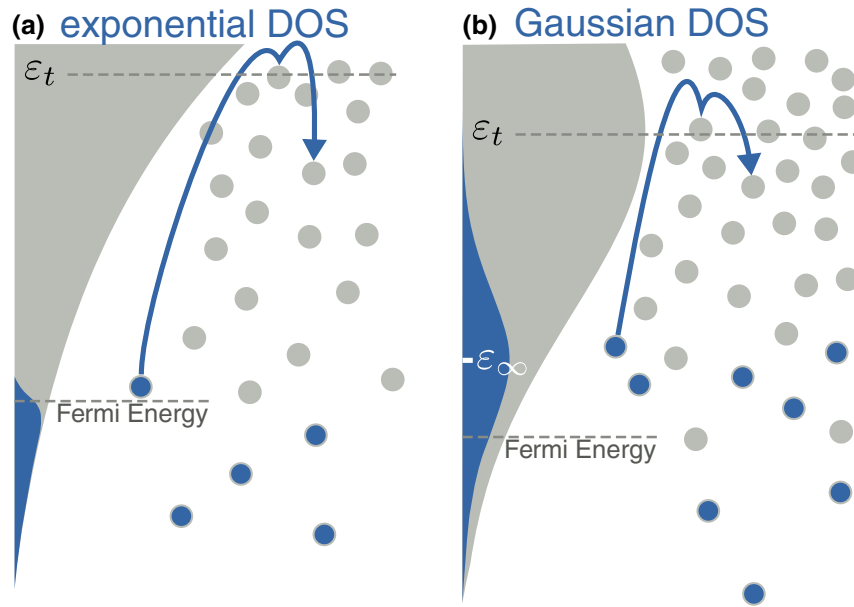


Figure 4. Schematic picture of the equilibrium carrier distribution in the exponential (a) and Gaussian (b) DOS. Occupied states are marked blue.

if carriers are artificially forced only to hop to the nearest neighbours in simulation algorithms or in analytical studies. It is particularly erroneous at low temperatures, when the characteristic hopping length in reality exceeds the nearest-neighbour spacing (the VRH regime), while the carriers in the modeling are forced to move only via short hops to the nearest neighbours on the grid [74, 75]. Constraining the model to the nearest-neighbour transitions on a lattice is also not correct in the case of high temperatures, when charge transport occurs in the NNH regime, since the results of the modeling depend essentially on the choice of the particular lattice structure [74, 75], while the real disordered media can hardly recall a regular lattice grid. Therefore, even in the case of the NNH when the typical hopping length is of the order of the inter-site distance, one should always consider spatially random systems.

3.3. Gaussian DOS against exponential DOS

If the thermal energy kT is smaller than the energy scale of disorder σ , which is the case for ODSs, where at room temperature $kT \approx 0.3\sigma$ [9, 24], charge transport occurs in the VRH regime, i.e. the interplay between the spatial and energy factors determines the transport path. Under these circumstances, the shape of the energy spectrum plays the crucial role for charge transport and the decisive task is to determine the DOS for the underlying material. Exponential DOS given by equation (4) or Gaussian DOS given by equation (3) are most often used in the literature for ODSs and it is claimed sometimes [41] that there is no principle difference between the steeply energy-dependent DOS functions in their ability to describe charge transport, particularly to account for the dependence of carrier mobility μ on the concentration of carriers n . Below we show that, on the contrary, the shape of the dependence $\mu(n)$ for the exponential DOS given by equation (4) is not only quantitatively, but also

qualitatively different to that for the Gaussian DOS given by equation (3). Herewith we claim that studying the dependence $\mu(n)$ experimentally one can distinguish between these two possible shapes of the DOS.

In order to understand this message, one should clarify what is different and what is similar for charge transport in the case of Gaussian DOS as compared to the case of exponential DOS. As will be shown in sections 5 and 6, transport in both cases is dominated by thermally activated transitions of charge carriers towards the energy level ε_t situated far above the energy region occupied by carriers. This feature is qualitatively similar for all steeply energy-dependent DOS functions. The position of the level ε_t , traditionally called the *transport energy*, depends slightly on the shape of the DOS. What is, however, qualitatively different in the case of Gaussian DOS, as compared to the case of the exponential DOS, is the kind of thermal distribution of carriers along the energy spectrum of the system.

The distribution of carriers in thermal equilibrium is described by the product $g(\varepsilon)f(\varepsilon)$, where $g(\varepsilon)$ is the DOS and $f(\varepsilon)$ is the Fermi distribution,

$$f(\varepsilon) = \left[1 + \exp \left(\frac{\varepsilon - \varepsilon_F}{kT} \right) \right]^{-1}. \quad (17)$$

In the exponential DOS given by equation (4), the maximum of the carrier distribution $g(\varepsilon)f(\varepsilon)$ at $kT < \varepsilon_0$ is in close vicinity of the concentration-dependent Fermi energy $\varepsilon_F(n)$, as illustrated schematically in figure 4(a). Mobility, determined by carrier activation from $\varepsilon_F(n)$ towards ε_t is therefore always a function of n , as schematically illustrated by the dashed line in figure 6.

In the Gaussian DOS, on the contrary, most carriers at low n are distributed not around the Fermi level, but are instead situated around the so-called *equilibration energy* ε_∞ . This

energy is usually identified with the average carrier energy determined as [9, 77]

$$\varepsilon_\infty = \frac{\int_{-\infty}^{\infty} \varepsilon g(\varepsilon) \exp(-\varepsilon/kT) d\varepsilon}{\int_{-\infty}^{\infty} g(\varepsilon) \exp(-\varepsilon/kT) d\varepsilon} = -\frac{\sigma^2}{kT}. \quad (18)$$

Here we follow the traditional definition of ε_∞ via equation (18) [9], since for the Gaussian DOS given by equation (3) the maximum of the product $g(\varepsilon)f(\varepsilon)$ corresponds to ε_∞ given by equation (18). This situation, with most carriers occupying in thermal equilibrium energy levels far above the Fermi level, is counter-intuitive. It occurs because the number of states in the Gaussian DOS increases above the Fermi level at a much steeper rate than the decrease of the occupation probability described by the Fermi function. The distribution of carriers in the Gaussian DOS at low n is illustrated schematically in figure 4(b). In such a case, transport in the Gaussian DOS is due to carrier transitions via energy levels in the range between ε_∞ and ε_t . Neither of these energies depend on the concentration of carriers n . Furthermore, the occupation numbers of states in the range between ε_∞ and ε_t is very low, $f(\varepsilon) \ll 1$ and the carriers can be considered as independent from each other (filling of states in the range between ε_∞ and ε_t can be neglected). Therefore, the carrier mobility in the Gaussian DOS at low n does not depend on n , which is in striking contrast to the situation in the exponential DOS, where carrier mobility depends on n at all n values.

This picture with most carriers occupying energy levels around ε_∞ in the Gaussian DOS is valid at low n , when the Fermi energy $\varepsilon_F(n)$ is far below the equilibration energy ε_∞ . With rising n , the Fermi energy $\varepsilon_F(n)$ moves upwards and it crosses ε_∞ at a carrier concentration n_c determined by the equation [67, 69, 72]

$$\varepsilon_F(n_c) = \varepsilon_\infty, \quad (19)$$

where the Fermi energy $\varepsilon_F(n)$ is determined via the relation

$$\int_{-\infty}^{\infty} g(\varepsilon) f(\varepsilon, \varepsilon_F) d\varepsilon = n. \quad (20)$$

In figure 5, the crossing between ε_F and ε_∞ with varying n is illustrated schematically [78].

Since both ε_∞ and ε_F depend on temperature T , the criterion given by equation (19) can also be treated as a function of T rather than of the carrier concentration:

$$\varepsilon_F(T_c, n) = \varepsilon_\infty(T_c). \quad (21)$$

In fact, this temperature-dependent form was suggested first [67] and only later reformulated in the form of equation (19) [38, 69, 72].

The dependence $\mu(n)$ is shown schematically in figure 6 for the exponential and Gaussian DOS. It is clearly visible that the mobility in the Gaussian DOS is concentration-independent at low concentrations $n < n_c$ and becomes dependent on n at $n > n_c$, whereas the carrier mobility in the exponential DOS depends on n at all concentrations. A concentration-independent mobility at low n was observed experimentally for

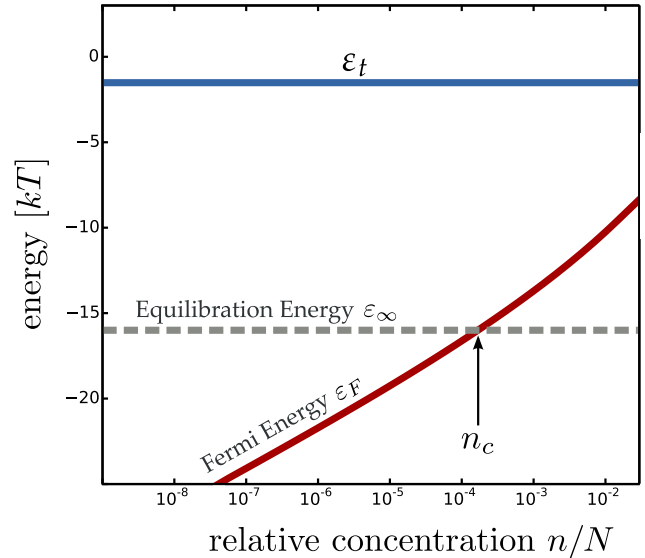


Figure 5. Positions of the concentration-dependent Fermi energy ε_F given by equation (20) and of the equilibration energy ε_∞ given by equation (18) at $\sigma/kT = 4$. Position of the transport energy ε_t is calculated via equation (60).

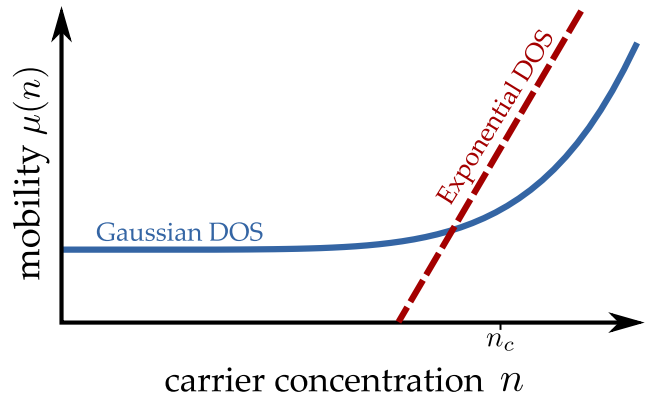


Figure 6. Schematic dependences of the carrier mobility on concentration of carriers n in a Gaussian DOS (solid line) and in an exponential DOS (dashed line). Concentration n_c corresponds to the condition given by equation (19).

the widely studied ODSs PPV and P3HT [43, 79], which is a strong indicator for these materials possessing a DOS steeper than a purely exponential one. Mobility independent of the concentration n at low n was also found for three derivatives of quinquethiophenes (5T) [80, 81]. It is worth emphasizing once more that the independence of the carrier mobility on n at low carrier concentrations n clearly rules out the exponential DOS as a candidate for such materials, whereas the measured data fit perfectly into the GDM picture [19, 38, 67, 69, 72, 78].

Note, that ε_∞ can be found in any DOS decaying steeper than purely exponentially and the threshold concentration n_c can be calculated via equation (19). Concomitantly, the plateau of $\mu(n)$ at $n < n_c$ is to be found for any of these steep DOS functions. Moreover, the value of n_c drastically depends on the shape of the DOS, as shown in the detailed study by Oelerich *et al* [38]. Comparison between n_c from equation (19) and the experimental data for PPV and P3HT from [43] indicates that

these materials possess a DOS very close to the Gaussian one. Note also, that equation (19) is not only valid in the GDM, but should hold for systems with space-energy correlations, i.e. for the CDM.

In the following sections, we present several theoretical tools to describe hopping charge transport in ODSs.

4. WoT: percolation theory

The most successful theoretical approach among those developed so far to describe the VRH and NNH in disordered systems is the *percolation theory*. Therefore we start exploring the WoT by discussing this particular approach.

The basis for applying percolation theory to analyze hopping transport is the concept of the *resistance network* suggested by Miller and Abrahams [25]. In this concept, each site is modeled by a node of an electrical circuit and for each pair of sites (i, j), between which carrier jumps are possible, a resistance R_{ij} connecting the corresponding nodes is introduced. Then, the resistance of the whole sample can be found as the resistance of the equivalent network constructed from the elements R_{ij} . The values of R_{ij} are defined as [73, 82]

$$R_{ij} = \frac{kT}{e^2 \Gamma_{ij}}, \quad (22)$$

where $\Gamma_{ij} = v_{ij} f(\varepsilon_i)[1 - f(\varepsilon_j)]$ is the equilibrium rate of carrier transitions from site i to site j . According to the detailed balance principle, $\Gamma_{ij} = \Gamma_{ji}$. For the case of MA hopping rates, the values of Γ_{ij} are given by equations (8) and (17).

It is crucial for evaluating the network resistance that the magnitudes of R_{ij} are distributed in an exponentially broad range. (This can be easily seen from equation (8), keeping in mind that the scatter of hop lengths r_{ij} is, typically, large as compared to the localization length α and the distribution of site energies has a width much larger than kT .) In such conditions, very large resistances do not contribute to transport because they can be bypassed through paths with much lower resistances. On the other hand, resistances of very small values serve simply as short-cuts between larger resistances, hence their exact values are not important. These simple arguments give a hint that there is such a ‘critical’ value R_{crit} that pairs of sites with $R_{ij} \gg R_{\text{crit}}$ and with $R_{ij} \ll R_{\text{crit}}$ do not play a decisive role for the overall conductivity of the network.

Percolation theory provides a precise meaning for R_{crit} via the following arguments [73]. Let us sequentially delete resistors from the network, starting from the largest one and proceeding in the order of descending resistances. At some ‘critical’ step in this procedure, deleting the next resistor disconnects the opposite sides of the sample. Then, R_{crit} is, by definition, the resistance of the element deleted at this ‘critical’ step, taken in the limit of an infinitely large sample. The corresponding value R_{crit} determines the main (exponential) factor in the macroscopic resistivity [73]. As we will see below, in the most important cases the evaluation of R_{crit} can be reduced to purely geometrical problems of the percolation theory. Also the slowly varying pre-exponential factor, which

appears in resistivity along with R_{crit} , can be estimated on the basis of the percolation theory [73].

In section 4.1 we will apply the percolation approach to the simplest model of isoenergetic sites. Then, in sections 4.2–4.4 we will consider the low-temperature conductivity described by the Mott law and the transport in systems with exponential and Gaussian DOS. If not specified otherwise, we will assume the MA transition rates given by equation (8).

4.1. Percolation theory for the NNH with isoenergetic sites

Let us consider hopping transport via localized states, which are randomly distributed in 3D space and possess equal carrier energies. We assume strong localization, implying that the localization length α is small as compared to the typical distance between sites $N^{-1/3}$, where N is the concentration of sites. In real systems, this model can be relevant at high enough temperatures, when kT is larger than the characteristic energy scale of the DOS. In this case, elementary resistances R_{ij} differ from each other only due to the different distances r_{ij} between sites: $R_{ij} = R_0 \exp(2r_{ij}/\alpha)$, where the prefactor R_0 is the same for all pairs of sites. We will consider R_0 as constant while varying the site concentration, which means keeping the fraction of occupied sites unchanged.

Finding the critical resistance R_{crit} is reduced to the following purely geometrical problem. Let us consider a pair of sites as connected if the distance between the sites is less than some fixed value r . When r is large enough, connected pairs form an *infinite cluster*, i.e., there exists a path over the whole structure passing only through connected pairs of sites. At small values of r , only finite clusters of connected sites can exist. Let r_c be the smallest value of r at which the infinite cluster still exists. Then,

$$R_{\text{crit}} = R_0 \exp(2r_c/\alpha). \quad (23)$$

The quantity r_c depends on the concentration of sites N . It is convenient to express r_c through a dimensionless parameter B_c —an average number of sites within the sphere of radius r_c around a given site [73, 83, 84]:

$$\frac{4\pi}{3} N r_c^3 = B_c. \quad (24)$$

As a dimensionless quantity, B_c does not depend on N ; thus, its value is universal: $B_c \cong 2.735$ [85]. Since r_c does not depend on temperature, the NNH regime is valid for this model of conduction.

Let us consider the dependence of the dc conductivity σ_{dc} through isoenergetic sites on their concentration N . This dependence is exponentially strong, because the concentration-dependent value r_c appears in the exponent in equation (23). From equations (23)–(24) one can express σ_{dc} as follows [73]:

$$\sigma_{\text{dc}}(N) \propto R_{\text{crit}}^{-1} \propto \exp\left(-\frac{2r_c}{\alpha}\right) \equiv \exp\left(-\frac{\gamma N^{-\frac{1}{3}}}{\alpha}\right), \quad (25)$$

where $\gamma = 2(3B_c/4\pi)^{1/3} \cong 1.7351$ according to equation (24).

Equation (25) provides a solid basis for the understanding and quantitative analysis of the concentration dependence of

σ_{dc} in systems with low concentration of localization sites ($N^{-1/3} \gg \alpha$) at high temperatures. Notably, equation (25) shows that the conductivity monotonously decreases with decreasing N . Hence, there is no such threshold concentration N_c (often assumed in ODSs) that σ_{dc} strictly vanishes at $N < N_c$.

It is possible to go beyond equation (25) and to estimate also the non-exponential factors in the expression for σ_{dc} . The key point is that adding pairs with $R_{crit} < R_{ij} \leq R_{crit} \exp(\delta)$, where $\delta \simeq 1$, to the percolation cluster gives the major contribution to the conduction [73]. The infinite cluster formed by this set of pairs, the so-called ‘critical subnetwork’ [73], or ‘fat percolation cluster’ [86], determines the conductivity. An important characteristic of the critical subnetwork is its correlation length L_{corr} , which possesses the following feature: on length scales larger than L_{corr} the subnetwork can be considered homogeneous, whereas on smaller scales it is highly inhomogeneous [73]. As explained in section 5.6 of the monograph by Efros and Shklovskii [73], one can estimate the conductivity σ_{dc} of the resistor network in the 3D case via the relation

$$\sigma_{dc} \simeq R_{crit}^{-1} L_{corr}^{-1}. \quad (26)$$

The correlation length, in turn, depends on the fraction ϵ of pairs with resistances above R_{crit} , in the manifold of the resistors added in order to form the critical subnetwork. When ϵ is small, L_{corr} is proportional to $\epsilon^{-\nu}$, where ν is the universal critical index of the correlation length of the percolation cluster. In 3D, $\nu = 0.875 \pm 0.008$ [87]. Since in the system of isoenergetic sites $\epsilon \simeq \alpha/r_c \simeq \alpha N^{1/3}$, the correlation length of the critical subnetwork depends on α as

$$L_{corr} \propto (\alpha N^{1/3})^{-\nu}. \quad (27)$$

Finally, collecting equations (23)–(27) one can obtain the following expression for the conductivity σ_{dc} in 3D case:

$$\sigma_{dc}(N) = A R_0^{-1} N^{\frac{1}{3}} (\alpha N^{\frac{1}{3}})^{\nu} \exp\left(-\frac{\gamma N^{-\frac{1}{3}}}{\alpha}\right), \quad (28)$$

where $\gamma \approx 1.735$, $\nu \approx 0.875$ and A is a numerical coefficient of order unity. The dependence $\sigma_{dc}(N)$ over several orders of magnitude has been observed in numerous experimental studies of hopping transport via impurity atoms in doped crystalline semiconductors, where the values of the localization length α for randomly placed impurities are well known [73]. The prefactor R_0 may depend on hopping distance. If so, one should use the value of R_0 at r_c .

4.2. Percolation theory for the VRH, Mott law

Let us now turn to considering the VRH transport regime, which, as explained in section 3.1, comes in to play when kT is smaller than the characteristic width of the DOS. Analysis of the VRH conduction in the framework of the percolation theory is more sophisticated than in the NNH case, because the dependence of transition rates on site energies also turns out to be essential, along with the dependence of transition

rates on the intersite distances. One can consider the charge transport in these conditions as percolation in 4D space, whose coordinates are three spatial axes and the energy. In this context, an important question arises: is it still possible to analyze the charge transport in the VRH regime in terms of the average number of bonds B_c given by equation (24), or is it necessary to go beyond this simple approach?

In the current subsection we focus on the temperature dependence of the conductivity at very low temperatures, when transport occurs only in close vicinity of the Fermi level ϵ_F . As explained in [73], this dependence can be found as a solution of a 4D percolation problem yielding the prominent Mott law. The corresponding 4D percolation problem looks as follows. Consider a set of points randomly placed in 3D space with some given concentration. Each point is characterized by its dimensionless position vector $\tilde{\mathbf{r}}_i$ and a dimensionless ‘energy’ $\tilde{\epsilon}_i$. The latter quantity is uniformly distributed in the range $[-1, 1]$. Two points i and j are considered as connected if

$$\frac{|\tilde{\epsilon}_i| + |\tilde{\epsilon}_j| + |\tilde{\epsilon}_i - \tilde{\epsilon}_j|}{2} + |\tilde{\mathbf{r}}_i - \tilde{\mathbf{r}}_j| \leq 1. \quad (29)$$

The problem is to find the minimal concentration \tilde{n} , at which the connected system of points forms an infinite percolation cluster. Below we will assume that the concentration of points is fixed at this threshold value \tilde{n} .

Let us further introduce a spatial scale D and an energy scale W , connected to each other as

$$\frac{W}{kT} = \frac{2D}{\alpha} \quad (30)$$

(the exact values of D and W will be determined later). One should keep in mind that each point i is associated with a site in a real sample, located at

$$\mathbf{r}_i = D \tilde{\mathbf{r}}_i \quad (31)$$

and having the energy

$$\epsilon_i = W \tilde{\epsilon}_i + \epsilon_F. \quad (32)$$

These sites are uniformly distributed within the energy range $[\epsilon_F - W, \epsilon_F + W]$ and their concentration is equal to \tilde{n}/D^3 . The density of states around the Fermi level is therefore

$$g(\epsilon_F) = \frac{\tilde{n}}{2W D^3}. \quad (33)$$

The connection criterion (29) corresponds to the following relation between sites i and j :

$$\frac{|\epsilon_i - \epsilon_F| + |\epsilon_j - \epsilon_F| + |\epsilon_i - \epsilon_j|}{2kT} + \frac{2r_{ij}}{\alpha} \leq \frac{W}{kT}. \quad (34)$$

Using equations (8) and (22), one can rewrite this criterion as

$$R_{ij} \leq \frac{kT}{e^2 \nu_0} \exp\left(\frac{W}{kT}\right). \quad (35)$$

Since the criterion given by equation (29) provides the percolation threshold by construction, the same is true for equation (35), i.e. pairs of sites obeying equation (35) form

the least dense infinite cluster. Hence, the critical value of the resistance R_{crit} is equal to the r. h. s. of equation (35). (Note that, for finding R_{crit} , it is sufficient to take into account only sites with energies in the range $[\varepsilon_F - W, \varepsilon_F + W]$, because all other sites do not satisfy the inequality (34).) Hence, the conductivity σ_{dc} scales as

$$\sigma_{\text{dc}} \propto R_{\text{crit}}^{-1} \propto \exp(-W/kT), \quad (36)$$

where W is the half-width of the energy strip around ε_F , in which conduction takes place. The value of W can be found by resolving the system of equations (30) and (33) with respect to W and D :

$$W = kT [(T_0/T)^{1/4}], \quad (37)$$

where $T_0 = \beta/[kg(\varepsilon_F)\alpha^3]$ and $\beta \equiv 4\tilde{n}$ is a numerical factor that can be obtained from the solution of the dimensionless percolation problem described above. The energy scale for the most important hops decreases with decreasing temperature ($W \propto T^{3/4}$) and simultaneously the spatial scale increases ($D \propto T^{-1/4}$). This indicates the VRH character of the conduction: at smaller temperatures, the carrier chooses more distant hops in order to reduce the difficulty of overcoming the energy barrier.

Equations (36) and (37) give the prominent Mott law [88] for the temperature dependence of hopping conductivity:

$$\sigma_{\text{dc}} = \sigma_{\text{dc}}^0 \exp[-(T_0/T)^{1/4}], \quad (38)$$

where the prefactor σ_{dc}^0 only weakly (non-exponentially) depends on temperature. It is worth emphasizing that the percolation approach is capable of evaluating this prefactor, up to a constant factor of the order unity. One can find the details in section 9.4 of [73]. The above consideration shows that the Mott law (38) is valid when the DOS can be considered as constant in the energy range $\varepsilon_F \pm W$.

4.3. Percolation theory for the VRH in the case of exponential DOS

As mentioned in section 1, as early as the 1970s and 1980s, a comprehensive theory of the VRH was developed for systems with the purely exponential DOS given by equation (4) and we first focus on this shape of the DOS. For the exponential DOS, the Mott law is valid at temperatures satisfying the strong inequality $kT(T_0/T)^{1/4} \ll \varepsilon_0$. Using the estimate $g(\varepsilon_F) \approx n/\varepsilon_0$ for concentration of carriers n , one obtains the condition $kT/\varepsilon_0 \ll (n\alpha^3)^{1/3}$ for the validity of the Mott's law.

In 1979, Grünewald and Thomas [89] used percolation theory to study the VRH in the exponential DOS at temperatures above the validity range of the Mott law and discovered a new regime, in which the carrier mobility is described as

$$\mu = \frac{\sigma_{\text{dc}}}{en} = \frac{\sigma_{\text{dc}}^0}{en} \exp\left[-\frac{\varepsilon^* - \varepsilon_F(n, T)}{kT}\right], \quad (39)$$

where σ_{dc}^0 is the preexponential factor in the expression for the conductivity and ε^* is the characteristic highest energy of sites

contributing to charge transport [89]. Unlike the Mott law, in this new regime the energy ε^* is fully detached from the Fermi level and does not depend on n .

Two decades later, the very same problem was addressed by the community working with ODSs [41]. While Grünewald and Thomas [89] in 1979 used the classical percolation approach [82, 90, 91], Vissenberg and Matters in 1998 used a 'somewhat different approach' [41] to that by Grünewald and Thomas. It is instructive to find out what was different and which of the two approaches gives more accurate results.

According to the percolation approach one first rewrites the rate given by equation (8) in the form

$$v_{ij} = v_0 \exp(-\xi_{ij}) \quad (40)$$

and determines $B(\varepsilon_i, \xi)$, the average number of sites accessible from a site with energy ε_i using hopping rates with the exponent ξ_{ij} smaller than some value ξ . The aim is to find out the magnitude of the exponent ξ_c that provides the infinite percolation path for carriers through the system of sites using only rates with $\xi \leq \xi_c$. In order to determine ξ_c , it is necessary to formulate the percolation criterion that relates the quantity $B(\varepsilon_i, \xi)$, appropriately averaged over site energies, to some numerical factor given by the percolation theory [82, 90, 91].

In a first approximation one might perform the averaging over site energies ε_i ascribing equal weights for all sites in the range $\varepsilon_F - kT\xi_c \leq \varepsilon_i \leq \varepsilon_F + kT\xi_c$ leading to the equation

$$B_c = \frac{\int_{\varepsilon_F - kT\xi_c}^{\varepsilon_F + kT\xi_c} d\varepsilon g(\varepsilon) B(\varepsilon, \xi_c)}{\int_{\varepsilon_F - kT\xi_c}^{\varepsilon_F + kT\xi_c} d\varepsilon g(\varepsilon)}, \quad (41)$$

where B_c is equal to that in equation (24). It is this way of averaging that was used by Vissenberg and Matters [41] for the exponential DOS (and later by Coehoorn *et al* [92] for the Gaussian DOS).

Close inspection performed by Pollak [91] and by Overhof [93] shows, however, that it is necessary for the averaging to use a weighting factor that is proportional to the average number of bonds for a given site energy ε , which leads to the percolation criterion [91, 93, 94]

$$B_c = \frac{\int_{\varepsilon_F - kT\xi_c}^{\varepsilon_F + kT\xi_c} d\varepsilon g(\varepsilon) B^2(\varepsilon, \xi_c)}{\int_{\varepsilon_F - kT\xi_c}^{\varepsilon_F + kT\xi_c} d\varepsilon g(\varepsilon) B(\varepsilon, \xi_c)}. \quad (42)$$

It is this way of averaging that was applied by Grünewald and Thomas [89] for the exponential DOS (and later by Baranovskii *et al* [67] for Gaussian DOS).

Remarkably, one can check which of the two percolation criteria is more accurate for the case of the exponential DOS. The exponential DOS, although probably not relevant for all ODSs [24, 38], is still useful as a test field for analytical and numerical methods, because its VRH problem can be solved exactly. Nenashev *et al* [95] recently showed that the four-dimensional (three spatial dimensions and energy) VRH problem in the exponential DOS can be mapped onto

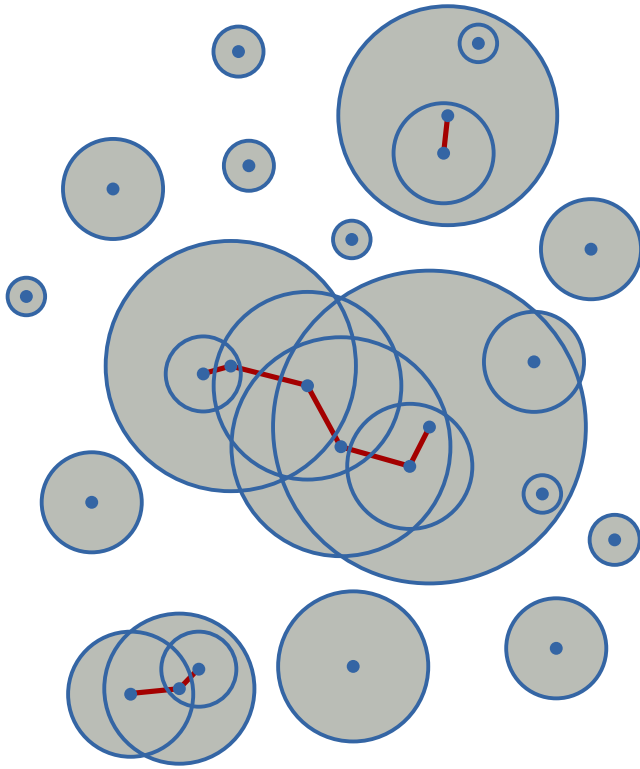


Figure 7. The system of spheres with exponentially distributed radii. Two spheres are considered connected, if the center of each of them lies within the other sphere. Paths between connected spheres are marked as red lines.

a purely geometrical problem of percolation via spheres with exponentially distributed radii. The latter problem is solvable exactly and provides not only the exponential dependence of the conductivity on system parameters, but even the pre-exponential factors with much weaker dependences [95]. This mapping is possible at the reasonable condition $\epsilon_0 > kT$. In this case, one can show that the percolation problem in a 3D system of randomly placed spheres with radii distributed via $g(r) = N \exp(-\tilde{r})$ (\tilde{r} being a dimensionless radius) represents the 4D VRH problem. This percolation problem is schematically shown in figure 7. The critical concentration \tilde{N}_c of spheres in this 3D problem is accessible numerically with high precision, yielding the result $\tilde{N}_c \approx 0.219$ [95]. This result can now be converted back into an accurate solution of the initial VRH problem.

The comparison between the results of Grünewald and Thomas [89], those obtained by Vissenberg and Matters [41] and the exact solution by Nenashev *et al* [95] is shown in figure 8. In addition, the figure contains a solution based on the transport energy (TE) concept, as suggested by Oelerich *et al* [38] (this approach is described in detail in section 5). All the analytical solutions shown in figure 8 can be presented in the form

$$\mu = \mathbf{A} \frac{v_0 e}{n \epsilon_0 \alpha} \left[\mathbf{B} \frac{n}{8} \left(\frac{\alpha \epsilon_0}{kT} \right)^3 \right]^{\epsilon_0/kT}, \quad (43)$$

with **A** and **B** being slowly varying or constant factors that differ between the solutions. The values of **A** and **B** are listed in table 1. The exponential dependences on the system

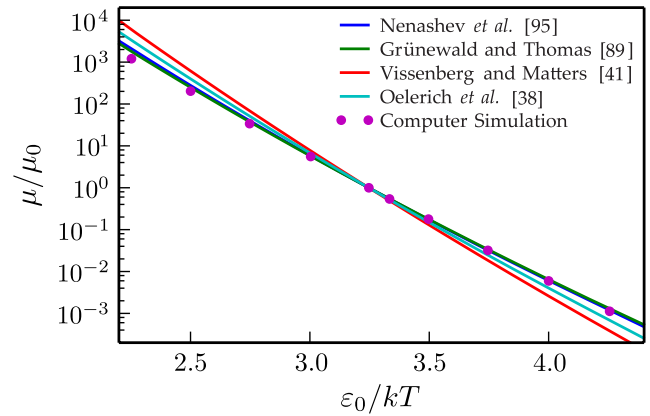


Figure 8. Normalized mobility values obtained from computer simulation and from equation (43) for the different analytical solutions, at $N^{1/3}\alpha = 0.3$ and $n/N = 0.001$. Reproduced with permission from [95]. Copyright 2013 by the American Physical Society.

Table 1. Values of **A** and **B** in equation (43) for the different compared expressions for the mobility μ . \tilde{C} is an unknown numerical coefficient, $\nu \approx 0.875$ and $\tilde{N}_c \approx 0.219$ are known from percolation theory [87, 95] and $B_c = 2.7$ is a percolation threshold taken from [73]. Reproduced with permission from [24].

Article	A	B
Nenashev <i>et al</i> [95]	$0.36 \left(\frac{kT}{\epsilon_0} \right)^\nu$	$\frac{1}{\tilde{N}_c}$
Oelerich <i>et al</i> [38]	$\frac{B_c}{2\tilde{C}}$	$\frac{4\pi}{3B_c} \frac{27}{\exp(3)}$
Vissenberg and Matters [41]	\tilde{C}	$\frac{\pi}{B_c}$
Grünewald and Thomas [89]	$\frac{1}{3}$	$\frac{B_c}{4\pi} \frac{68}{3B_c} \frac{68}{27}$

parameters in equation (43) are the same in all approaches. Note, that equation (43) is not valid for the low temperatures, when criterion $kT/\epsilon_0 > (n\alpha^3/8\tilde{N}_c)^{1/3}$ is violated [95]. All solutions are therefore restricted to temperatures above those, at which the well-known Mott law, given by equation (38), is expected.

In figure 8 the data for each of the four approaches is normalized to its value at $kT = 0.3\epsilon_0$. The deviations between the solutions are therefore only due to different temperature dependences. It is clearly visible from the figure that the result by Grünewald and Thomas [89] and the exact one by Nenashev *et al* [95] agree almost perfectly and match the simulation results very well. This is remarkable since the solution by Grünewald and Thomas was not only the first theory for the VRH in the exponential DOS based on the percolation theory, but it also uses a very simplistic approach with a percolation threshold $B_c = 2.7$ for overlapping spheres with equal sizes, which so far is proven valid only in the case of the NNH. The TE concept, which is introduced in section 5, performs slightly worse, but it still provides a good approximation for the temperature dependence. The solution by Vissenberg and Matters [41] shows the least agreement with the exact result and the computer simulations, although the deviations are still not large.

Regarding the different averaging procedures in equations (42) and (41), one can conclude that the classical averaging, as suggested by Pollak [91], is supported by the perfect

agreement between the theory of Grünewald and Thomas [89] and the exact solution by Nenashev *et al*. This averaging was also used by Baranovskii *et al* [67] for the Gaussian DOS. It is worth emphasizing once again that when dealing with percolation approaches, which rely on the critical number of bonds per site as a percolation criterion, it is important to carefully select the averaging procedure.

4.4. Percolation theory for the VRH in the framework of the Gaussian Disorder Model (GDM)

Percolation theory for the VRH in systems with Gaussian DOS has not yet been developed to the extent achieved in the case of exponential DOS, for which the physical problem has been converted into an exactly solvable geometrical one, as discussed in the previous section 4.3. Nevertheless, it is certainly possible to use percolation arguments to successfully describe the VRH in systems with a Gaussian DOS given by equation (3). Below we sketch this approach, closely following the arguments presented in [67, 68, 96].

Similar to the case of the exponential DOS, the Mott law is valid also for the Gaussian DOS at temperatures satisfying the strong inequality $kT(T_0/T)^{1/4} \ll \sigma$, where T_0 in equation (38) contains the same combination of parameters as in the case of the exponential DOS.

Let us show that the VRH regime described by equation (39) is also valid for the Gaussian DOS. In accordance with equation (8), the average number of sites $B(\varepsilon_i, \xi)$ accessible from a site with energy ε_i using hopping rates with the exponent ξ_{ij} smaller than some value ξ is equal to

$$B(\varepsilon_i, \xi) = \int d\varepsilon_j g(\varepsilon_j) \times \int d^3r_{ij} \theta\left(\xi - \frac{2r_{ij}}{\alpha} - \frac{\varepsilon_{ij}}{kT}\right), \quad (44)$$

with

$$\varepsilon_{ij} = [|\varepsilon_i - \varepsilon_j| + |\varepsilon_i - \varepsilon_F| + |\varepsilon_j - \varepsilon_F|]/2. \quad (45)$$

In order to determine the percolation path, these expressions should be inserted into equation (42) and the Gaussian DOS given by equation (3) should be used. The concentration of carriers n in any experimental situation is much smaller than the concentration of localized states N so that the Fermi level is situated in the low-energy part of the DOS and the lower half of the Gaussian DOS is relevant for charge transport. Due to the sharp increase of the Gaussian DOS above the Fermi level, the main contribution to the conductivity comes from the states with energies above the Fermi level. These energies are close to the upper edge of the conducting energy layer, $\varepsilon_F + \xi_c kT$ [96]. In this region (for $|\varepsilon_F + \xi_c kT|, \xi_c kT \gg \sigma$) the average number of bonds can be calculated exactly and from equation (42) one obtains the percolation criterion [96]

$$B_c = \frac{s^2}{6\sqrt{\pi}} \exp(-s^2), \quad (46)$$

where

$$s = \frac{\varepsilon_F + \xi_c kT}{\sqrt{2}\sigma}. \quad (47)$$

These equations lead to the percolation criterion for the Gaussian DOS:

$$\xi_c = \frac{\varepsilon_G^* - \varepsilon_F}{kT} \quad (48)$$

with

$$\varepsilon_G^* = -\sqrt{2}\sigma \ln^{1/2} Q, \quad (49)$$

$$Q = \frac{\gamma N \alpha^3}{B_c s_c^2} \left(\frac{\sigma}{kT}\right)^3, \quad (50)$$

where $s_c = -\ln[Q(s_c)]^{1/2}$ [67, 96].

Using equation (48) one obtains an equation similar to equation (39) for carrier mobility in the case of a Gaussian DOS:

$$\mu = \frac{\sigma_{dc}}{en} = \frac{\tilde{\sigma}_{dc}^0}{en} \exp\left[-\frac{\varepsilon_G^* - \varepsilon_F(n, T)}{kT}\right], \quad (51)$$

where $\tilde{\sigma}_{dc}^0$ is the pre-exponential factor in the expression for the conductivity independent from the carrier concentration n . Note, that the notation of ε_G^* in equation (51) was chosen to be different to that in equation (39), ε^* , in order to reflect the difference in DOS shapes used in their derivations. In the framework of the percolation theory, these energies appear as the highest energy levels which carriers have to achieve in order to perform long-range transport. More details regarding these energy levels will be discussed in section 5.

Although the functional forms of equations (39) and (51) look very similar to each other, the dependences of the mobility μ on the carrier concentration n and on temperature in the GDM are essentially different from those in systems with the exponential DOS, as discussed already in section 3.3. At $T > T_c$, or $n < n_c$, where n_c and T_c are given by equations (19) and (21), respectively, the Fermi level is situated below ε_∞ . In this regime, the Fermi energy can be approximated [67, 68, 96] as

$$\varepsilon_F(n, T) \simeq -\frac{1}{2} \frac{\sigma^2}{kT} - kT \ln\left(\frac{N}{n}\right). \quad (52)$$

Inserting this expression into equation (51) leads to the linear dependence of the exponential term in equation (51) on n and concomitantly to the remarkable result that carrier mobility does not depend on the concentration of carriers n at $n < n_c$ due to the presence of another n in the denominator in equation (51). This regime is in drastic contrast to the case of the exponential DOS, where the carrier mobility depends on the concentration of carriers n at all n values. Furthermore, inserting equation (52) into equation (51) shows that at $T > T_c$, or $n < n_c$, the temperature dependence of the mobility in the GDM has the form $\ln(\mu/\mu_0) \propto -(1/2)(\sigma/kT)^2$ [19, 24, 67, 97]. Often the dependence $\ln(\mu/\mu_0) \propto T^{-2}$ is considered as evidence for a Gaussian DOS, while the Arrhenius temperature dependence $\ln(\mu/\mu') \propto T^{-1}$ is claimed to indicate a purely exponential DOS. The important conclusion from the above consideration is the possibility of accounting for both kinds of temperature dependences of hopping conductivity in the framework of the

universal theoretical model based on the Gaussian DOS. The temperature dependence of the mobility is sensitive to the concentration of charge carriers n [19, 24, 67].

It was mentioned above that the VRH problem cannot be solved for a Gaussian DOS with the same precision as has been achieved for the exponential DOS, in the sense that in the latter case not only the exponential terms, but also pre-exponential factors in the expression for the conductivity can be obtained using the percolation theory [24, 95]. If one, however, simplifies the problem and considers not the real system of the randomly placed sites, as in the case of the VRH, but assumes that sites are placed on a regular grid and allows only transitions between the nearest neighbours, one can solve the percolation problem including the derivation of the pre-exponential terms in the expression for hopping conductivity for any shape of the DOS, including the Gaussian one [24, 73, 95].

The problem of transport on lattices was in fact solved several decades ago; the solution can be found in the monograph by Shklovskii and Efros [73]. By applying the method given in this monograph, one can show [95] that the mobility of charge carriers on a grid with lattice constant b is given by

$$\mu(T, n) \simeq \frac{e\omega_0}{kTbn} \left(\frac{kT}{\sigma}\right)^\nu \exp\left(\frac{\varepsilon_F(T, n) - \varepsilon^*}{kT}\right), \quad (53)$$

with the tunneling frequency $\omega_0 = v_0 \exp(-2b/\alpha)$. The energy level ε^* in this case can be obtained from the solution of the site percolation problem on a lattice. The number ν in equation (53) is the critical index of the correlation length of the percolation cluster already discussed in section 4.1. This number is universal in the sense that it does not depend on model parameters at scales shorter than the correlation length of the percolation cluster [73, 95]. Cottaar *et al* [74] recently found a similar solution for the GDM on a lattice. However, in that study, the numerical constant ν appears as a fit parameter depending on the lattice structure (SC or FCC) and on the choice of the hopping rates (Miller–Abrahams or Marcus equations). This example from the WoS once again shows that fitting of numerical results does not necessarily lead to correct conclusions.

5. WoT: the concept of the transport energy (TE)

The simple form of equation (51) might lead to the conclusion that the VRH in systems with Gaussian DOS takes place by activation of charge carriers towards the energy level ε_G^* . However, the r -dependent term in equation (8) plays an equally important role for the VRH as the thermal activation. Therefore, one can hardly assume that the description of the VRH as simple activation of carriers towards the energy level ε_G^* would mean that carriers actually conduct moving around that energy level. One should instead interpret the energy level ε_G^* in equation (51) as an ‘effective’ energy level serving formally to mimic the combined effects of the spatial tunneling and of the activation in energy. The role of ε_G^* is discussed in detail in section 6.3. Only in the case of the NNH, can the level

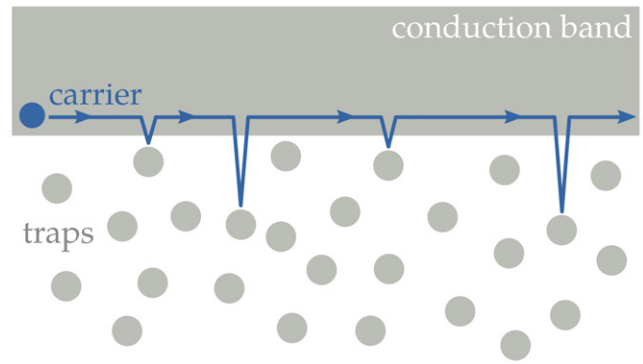


Figure 9. A sketch of the multiple-trapping process.

ε_G^* be treated as decisive for hopping conduction. Therefore, percolation theory is not a suitable tool to determine the ‘real’ energy path that charge carriers have to visit in order to provide transport in the VRH regime.

A powerful theoretical method for the description of hopping transport in systems with steeply energy-dependent DOS, complementary to the percolation theory, is the concept of the TE. Initially, this approach was developed for systems with the exponential DOS [98, 99] and was later extended for systems with other energy spectra, for instance, with a Gaussian DOS [100]. The essence of the TE approach is the ability to describe hopping transport via sites distributed in space and energy in full analogy with the multiple-trapping (MT) model by replacing the mobility edge in the MT model with a particular energy level ε_t [98–100].

The MT model was initially developed to describe charge transport in inorganic disordered materials, such as chalcogenide glasses and amorphous silicon [101–103], which possess the so-called mobility edge, i.e. the energy level that separates extended states with rather high carrier mobility from the localized states, which can be considered as traps. In the MT model, a charge carrier moves only via delocalized states with energies above the mobility edge. This motion is interrupted by trapping into localized states with subsequent activation of carriers back into the conducting states above the mobility edge. Transport in the framework of the MT model is shown schematically in figure 9. The advantage of the MT charge transport mode as compared to the VRH, is the possibility of exact theoretical treatment by analytical equations under equilibrium and non-equilibrium conditions for various shapes of the DOS [104–106].

There is some confusion in the literature with respect to the term ‘transport energy’. Mixing up the effective TE ε_G^* in equation (51) with the real TE ε_t is probably the main reason for that confusion. While the effective TE ε_G^* serves as a formal tool to describe the VRH as simple activation, the real TE ε_t characterizes the transport level at which carriers actually conduct. The difference between these effective and real TEs becomes more transparent if one compares the expressions for the mobility of charge carriers μ derived in various approaches. After deriving ε_t for the GDM [100] in full analogy with the derivations for the exponential DOS, Baranovskii *et al* [97] suggested the following expression for the carrier mobility at

$n \ll n_c$:

$$\mu = \mu_0 \exp \left[-\frac{2r(\varepsilon_t)}{\alpha} - \frac{\varepsilon_t}{kT} - \frac{1}{2} \left(\frac{\sigma}{kT} \right)^2 \right], \quad (54)$$

where $r(\varepsilon_t)$ is the typical distance between localized states with energies below ε_t . Working with the effective TE ε_{eff} , Arkhipov *et al* [107] and Nikitenko *et al* [108] suggested a slightly different expression for the carrier mobility:

$$\mu = \tilde{\mu}_0 \exp \left[-\frac{\varepsilon_{\text{eff}}}{kT} - \frac{1}{2} \left(\frac{\sigma}{kT} \right)^2 \right]. \quad (55)$$

Taking into account that values of μ_0 in equation (54) and $\tilde{\mu}_0$ in equation (55) are very close to each other [97, 107, 108], it is apparent that the meaning of the effective TE ε_{eff} is different to that of the TE ε_t . ε_{eff} in equation (55) is denoted differently to the energy ε_G^* in equation (51) particularly because the percolation nature of the VRH has not been taken into account in the derivation of ε_{eff} by Arkhipov *et al* [107] and by Nikitenko *et al* [108]. The same is true for the initial derivation of the ε_t in the GDM by Baranovskii *et al* [100]. Later Oelerich *et al* [78] derived the equation for ε_t in the GDM, taking into account the percolation criterion and extending this concept for finite carriers concentrations n . The dependence of the ‘effective’ transport energy, ε_{eff} on n has been derived by Arkhipov *et al* [109].

Another interesting definition of the TE was suggested by Schmechel [69], who, in contrast to all other derivations of the TE, did not use this quantity to calculate the carrier mobility, but instead derived the TE *from* the previously calculated dc conductivity by introducing a differential energy-dependent dc conductivity. The percolation nature of the cluster of sites responsible for the VRH has not been taken into account in that derivation.

Martens *et al* [110] essentially repeated the derivation by Baranovskii *et al* [100], also not taking into account the percolation nature of the VRH transport.

Studying different derivations of the transport energy, one should keep in mind that, not only is the value ε_t important, but so also is the way that it is used to calculate transport coefficients. One popular and transparent approach to obtain the TE is the optimization of hopping rates [78, 99, 100, 111]. Below we briefly describe this approach and point out how the carrier mobility can be obtained from the calculated ε_t .

5.1. Optimization approach to the TE

Consider a carrier in a state with energy ε_i . According to equation (1), the typical rate of a hop of this carrier to a site deeper in energy is

$$v_{\downarrow} = v_0 \exp \left[-\frac{2r(\varepsilon_i)}{\alpha} \right], \quad (56)$$

where

$$r(\varepsilon) = \left[\frac{4\pi}{3B_c} \int_{-\infty}^{\varepsilon} g(\varepsilon') d\varepsilon' \right]^{-1/3}. \quad (57)$$

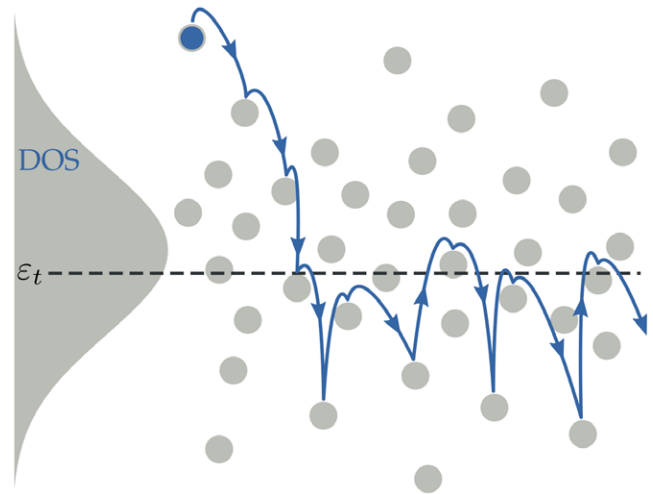


Figure 10. Schematic picture of carrier energy relaxation via the transport energy in an empty system with Gaussian DOS.

The factor B_c accounts for the percolation nature of hopping transport, i.e. the necessity for the hopping carrier to find a continuous path through the system, as discussed in detail in section 4. The rate of an activated jump of the carrier to a site with higher energy, $\varepsilon_x > \varepsilon_i$, is

$$v_{\uparrow}(\varepsilon_i, \varepsilon_x) = v_0 \exp \left[-\frac{2r(\varepsilon_x)}{\alpha} - \frac{\varepsilon_x - \varepsilon_i}{kT} \right]. \quad (58)$$

The transport energy ε_t is obtained from equation (58) by finding the most likely targeted energy in a hop from the level ε_i upwards in energy:

$$\frac{\partial v_{\uparrow}(\varepsilon_i, \varepsilon_t)}{\partial \varepsilon_t} = 0. \quad (59)$$

Inserting equations (57) and (58) into equation (59), one arrives at the following expression for the transport energy:

$$\exp \left(\frac{\varepsilon_t^2}{2\sigma^2} \right) \left[\int_{-\infty}^{\varepsilon_t/\sigma\sqrt{2}} e^{-t^2} dt \right]^{4/3} = (9\sqrt{2\pi} B_c^{-1} N\alpha^3)^{-1/3} \frac{kT}{\sigma}. \quad (60)$$

It can be easily shown [99, 100], that ε_t does not depend on the initial energy ε_i and is therefore a universal quantity for a given set of system parameters $N\alpha^3$ and σ/kT . Therefore, charge carriers situated at energies below ε_t will most probably be activated to energies in the vicinity of ε_t and carriers above ε_t will most probably fall down in energy. As soon as they reach energies below ε_t , the carriers will perform MT-like motion [112] with the mobility edge replaced by the TE ε_t [98–100]. Figure 10 schematically shows hopping transport within the GDM [97, 100].

A solution of equation (60) for reasonable values of parameters $\sigma/kT = 4$ and $N\alpha^3 = 0.01$ is shown in figure 5. The TE is situated in close vicinity of the maximum of the DOS, an assumption that can be found in previous studies [9, 113], yet without rigorous justification. Note, that the dependence of the TE on the charge carrier concentration was not taken into

account in the derivation of equation (60). This dependence will be introduced below in equation (64). It turns out that the TE is essentially independent of the concentration of charge carriers n up to rather high concentrations $n \approx 0.05 N$ [78].

It is important to find out how broad the distribution of the hopping rates is, or equivalently, how sharp the maximum calculated in equation (59) appears for reasonable parameter values. The energy width of the transport path around ε_t appears rather narrow [100]. As long as the distance between ε_t and the carrier distribution at ε_F or ε_∞ is larger than the energy scale of the DOS, σ , the TE model is an accurate tool for description of charge transport [38].

5.2. Numerical calculation of the TE

Along with many analytical approaches, the position of the transport energy was also studied using computer simulation techniques. Since the TE is, by most definitions, the energy path of conducting charge carriers, the first method that comes to mind is to simply trace the most frequently visited energies in straightforward computer simulations. This algorithm was suggested by Cleve *et al* [64] and used in several numerical studies [53, 114, 115]. Hartenstein and BäSSLer [114] recognized, however, that fast oscillations of carriers between localized states close in space and energy dominate the statistics of the most frequently targeted energies, though do not contribute to the long-range transport. This effect was addressed in analytical studies [116] and in computer simulations [53]. Comprehensive studies of such oscillations were provided by Mendels and Tessler [37] and by Oelerich *et al* [111], whose results clearly show that the algorithm suggested by Cleve *et al* can hardly be used to determine the position of the TE. More details can be found in [37, 111].

Oelerich *et al* [111] recently suggested a computer algorithm that allows one to determine the energy range that dominates the charge transport. The idea is to cut out sites with energies in an interval $[\varepsilon_{cut} - w, \varepsilon_{cut}]$ and to check whether the resulting mobility, determined in straightforward computer simulations, is affected by such a modification of the DOS. In figure 11 the corresponding modification is depicted. Charge carriers must avoid the sites with energies in this region and find other transport paths. Note, that the DOS is *not* renormalized after the modification. Depending on how much the withdrawn sites contribute to charge transport, the cutting will affect the mobility of the system more or less severely. The highest drop in the carrier mobility is expected when the cut-out sites are the most important ones for the long-range transport. This algorithm has been proven valid for revealing the position of the TE [111] by comparison with the exactly solvable hopping model, the NNH on a lattice.

In order to study the effect of the DOS modification for the case of the VRH, Oelerich *et al* [111] calculated the charge carrier mobilities using the balance equation approach [117, 118]. By varying the width w and the upper boundary ε_{cut} of the cutout interval (see figure 11), one can find at which w and ε_{cut} the maximal effect in the decrease of the carrier mobility is achieved and thereby reveal the energy range most important for charge transport. The data are presented in

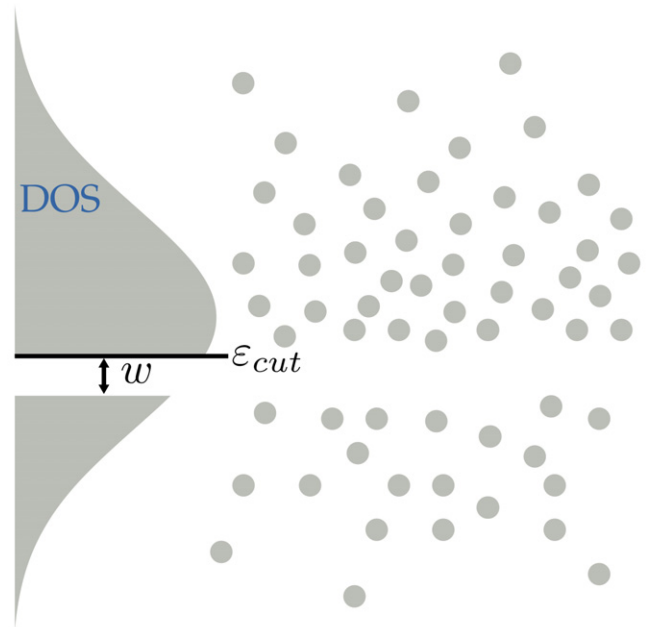


Figure 11. Schematic picture of the modified DOS $g(\varepsilon)$. Sites with energies in the interval $[\varepsilon_{cut} - w, \varepsilon_{cut}]$ are removed from the system.

figure 12. Results for two different widths, $w = 0.25\sigma$ and $w = 0.5\sigma$ at different temperatures kT are compared. In all cases, motion of a single charge carrier was simulated. The localization length was chosen as $\alpha = 0.215 N^{-1/3}$ and the number of sites in the simulated system was equal to 90^3 .

It is clearly visible in the figure that a significant decrease in the resulting mobility appears in each of the curves for a certain energy range of withdrawn sites. The effect is larger for larger energy intervals w , yet more accurate for lower values of w , since in that case the system is affected less severely. The choice of the interval width w should therefore be a compromise between the visibility of the effect and the accuracy in determining the position of the most efficient ε_{cut} . We interpret the minima on the curves plotted in figure 12 as pointing at the position of the real TE responsible for the long-range charge transport. The position of the TE, as determined from figure 12, shifts upwards in energy with rising temperature. This agrees with all previous analytical and numerical studies. The vertical lines close to the minima of the mobility curves in figure 12 show the positions of the TE calculated from equation (60). Apparently, the optimization approach leading to equation (60) is supported by the results of the straightforward computer simulations of the carrier mobility presented in figure 12.

Figure 12 also shows that when sites in the vicinity of the average carrier energy $\varepsilon_\infty = -\sigma^2/kT$ are cut out, the mobility is slightly increased. This happens for the following reason. In the Gaussian DOS in thermal equilibrium most carriers occupy sites around the equilibration energy ε_∞ . Removing sites around this energy pushes carriers to higher energies, decreasing the activation energy necessary for activation to the transport path, leading concomitantly to the increase of the carrier mobility.

The minima on the $\mu(\varepsilon_{cut})$ curves in figure 12, which we interpret as indicative for the real transport energy related to

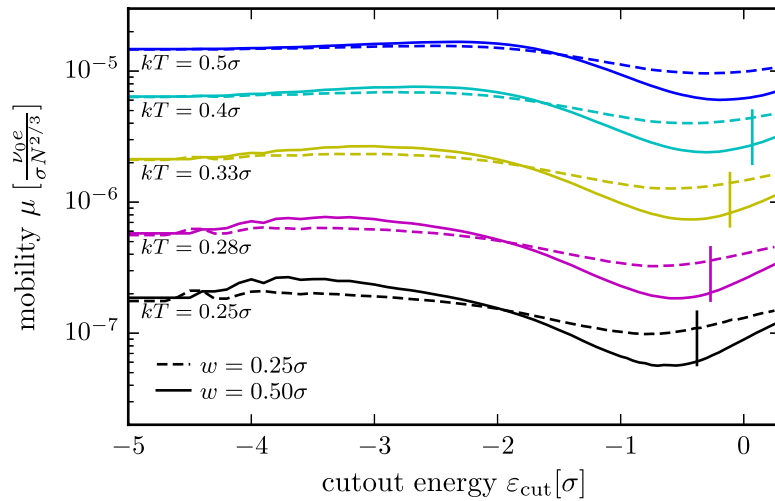


Figure 12. The mobility in a system with absent sites in the interval $[\varepsilon_{\text{cut}} - w, \varepsilon_{\text{cut}}]$. The vertical lines next to the minimum of the mobility are the analytical results for the transport energy from equation (60).

the long-range charge transport, are situated, for the given temperature range, close to the center of the DOS. It seems therefore correct to assume, in a simplified approach, that the TE coincides with the center of the Gaussian DOS, as has previously been suggested [9, 113]. It means that although charge carriers spend most time in states with energies around the equilibration energy $\varepsilon_{\infty} = -\sigma^2/kT$ transport takes place via sites with much higher energies than ε_{∞} .

The data in figure 12 show another remarkable feature, namely that cutting sites with energies in the vicinity of the level $-\sigma^2/2kT$ does not affect the carrier mobility significantly. This shows that it is wrong to interpret the VRH charge transport in the Gaussian DOS as activation of carriers from some particular energy level $\varepsilon_{\text{start}}$ to the transport energy ε_t . If the latter interpretation were correct, the observation of the mobility temperature dependence in the form of $\ln(\mu/\mu_0) \propto -1/2(\sigma/kT)^2$ [9] would yield the value of $\varepsilon_{\text{start}} \approx -\sigma^2/2kT$ for $\varepsilon_t \approx 0$. The fact that cutting sites with energies in the vicinity of the level $-\sigma^2/2kT$ does not affect the mobility means that this energy level does not play any significant role for the charge transport. The temperature dependence of carrier mobility in the form of $\ln(\mu/\mu_0) \propto -1/2(\sigma/kT)^2$ is instead the result of the time averaging over the upward hops to the TE from deeper energy levels [24, 38, 97].

From the above consideration one can conclude that for steeply energy-dependent DOS, such as the Gaussian or exponential DOS, the concept of the TE helps a lot to get a clear insight into the underlying physical processes responsible for charge transport. Using the concept of the TE, Oelerich *et al* [38] derived the equation for the VRH mobility in a system with a steeply energy-dependent DOS $g(\varepsilon)$ in the form

$$\mu \simeq v_0 \frac{e}{kT} \frac{3B_c F_{\text{ER}}}{4\pi r(\varepsilon_t) n_t} \times \exp\left(-\frac{2B_c^{1/3}}{\alpha} r(\varepsilon_t) - \frac{\varepsilon_t - \varepsilon_F}{kT}\right) \quad (61)$$

with n_t determined as

$$n_t = \int_{-\infty}^{\varepsilon_t} f(\varepsilon, \varepsilon_F) g(\varepsilon) d\varepsilon \quad (62)$$

and the function F_{ER} derived by Roichman and Tessler [119] in the form

$$F_{\text{ER}} = \frac{\int_{-\infty}^{\infty} d\varepsilon g(\varepsilon) \frac{\exp[(\varepsilon - \varepsilon_F)/kT]}{(1 + \exp[(\varepsilon - \varepsilon_F)/kT])^2}}{\int_{-\infty}^{\infty} d\varepsilon g(\varepsilon) \frac{1}{1 + \exp[(\varepsilon - \varepsilon_F)/kT]}} \quad (63)$$

The value of the TE ε_t is, in the general case, determined via the equation [24, 38]

$$\frac{2}{3} \left(\frac{4\pi}{3B_c}\right)^{-\frac{1}{3}} \frac{kT}{\alpha} \left[\int_{-\infty}^{\varepsilon_t} [1 - f(\varepsilon, \varepsilon_F)] g(\varepsilon) d\varepsilon \right]^{-\frac{4}{3}} \times [1 - f(\varepsilon_t, \varepsilon_F)] g(\varepsilon_t) = 1. \quad (64)$$

The function $r(\varepsilon)$ in the above equations is given by equation (57) and the factor $B_c = 2.735$ [85] accounts for the percolation nature of the hopping transport. Equation (64) is an extension of equation (60) that accounts for finite charge carrier concentrations.

Using equation (61) and (64), one obtains the data shown in figure 8 marked as Oelerich *et al* for the VRH mobility in the case of the exponential DOS given by equation (4) [38]. Comparison with the exact solution in figure 8 shows that equation (61) based on the TE concept is as accurate as the results based on the percolation approach and computer simulations.

6. WoT: mathematical solution for the VRH using the method of dissipated heat

As explained above, the appropriate transport regime at temperatures smaller than the energy scale of disorder, $kT \ll \sigma$, is the VRH, in which the interplay between the spatial- and energy-dependent terms in the hopping probabilities determines the transport path. Appropriate theoretical methods to account for this transport mechanism

are the percolation theory, described in section 4 and the approach based on the TE concept, described in section 5. In this section, we introduce another analytical method to study charge transport in the VRH regime based on calculating the distribution of dissipated heat. Following the classical recipe, the system will be considered as a resistor network [25, 73, 82, 90, 91].

The new approach is outlined in section 6.1. In section 6.2, it is used to derive information about hopping activation energies. The distribution of lengths of decisive hops is studied in section 6.3, providing a clear picture of the VRH nature of hopping conduction. In section 6.4 we show that the method of cutting out parts of the DOS, as outlined in section 5, indeed yields reliable information about the transport energy.

6.1. Response of a resistor network's conductance on variations of individual resistors' conductances

Let us consider a resistor network under some voltage U . The conductance of the resistor connecting sites i and j is denoted by G_{ij} . The relation of this quantity with the hopping transition rates and the resistor method in general is described in the monograph by Shklovskii and Efros [73]. Voltages U_{ij} and currents $I_{ij} = U_{ij}G_{ij}$ are determined by a system of Kirchhoff's equations including balance of currents at each site i ,

$$\sum_j I_{ij} = 0, \quad (65)$$

and connections between voltages U_{ij} , potentials φ_i, φ_j and electromotive forces \mathcal{E}_{ij} ,

$$U_{ij} = \varphi_i - \varphi_j + \mathcal{E}_{ij}. \quad (66)$$

(A proper expression for the electromotive forces reads $\mathcal{E}_{ij} = \mathbf{F} \mathbf{d}_{ij}$, where \mathbf{F} is the external electric field, \mathbf{d}_{ij} is the vector joining sites i and j . Periodic boundary conditions in the field direction are assumed.)

In order to relate the conductance G of the whole network to local quantities G_{ij}, U_{ij} , let us consider the power \mathbb{P} of Joule heat generating by the network. On the one hand, this power consists of powers P_{ij} produced by individual resistors (summation is over pairs of sites, each pair is counted only once),

$$\mathbb{P} = \sum_{(i,j)} P_{ij} \equiv \sum_{(i,j)} U_{ij}^2 G_{ij}. \quad (67)$$

On the other hand, \mathbb{P} can be expressed through the network's conductance G and the voltage U applied to the network (which is the sum of electromotive forces along a line connecting opposite edges of the network),

$$\mathbb{P} = U^2 G. \quad (68)$$

These two equations provide the relation between quantities G and G_{ij} .

Let us consider infinitely small variations of conductances G_{ij} ,

$$G_{ij} \rightarrow G_{ij} + \delta G_{ij}, \quad (69)$$

while electromotive forces \mathcal{E}_{ij} and concomitantly the voltage U , are fixed. We are interested in the relative change of the network's conductance $\delta G/G \equiv \delta(\ln G)$ due to these variations. In order to calculate this quantity, we will consider the variation $\delta\mathbb{P}$ of the total power \mathbb{P} . First, we will obtain this variation from equation (67):

$$\delta\mathbb{P} = \sum_{(i,j)} \delta(U_{ij}^2 G_{ij}) = 2 \sum_{(i,j)} U_{ij} G_{ij} \delta U_{ij} + \sum_{(i,j)} U_{ij}^2 \delta G_{ij}. \quad (70)$$

Let us show that the first sum in the right-hand side of equation (70) vanishes (This sum will be denoted below as S_1). Note that each term in this sum remains unchanged under swap of indices $i \leftrightarrow j$. This gives the possibility of representing the sum over non-repeating pairs of sites via double sum over all sites (where each pair is counted twice): $2 \sum_{(i,j)} \rightarrow \sum_i \sum_j$. So,

$$S_1 = \sum_i \sum_j U_{ij} G_{ij} \delta U_{ij} \equiv \sum_i \sum_j I_{ij} \delta U_{ij}. \quad (71)$$

According to equation (66),

$$\delta U_{ij} = \delta\varphi_i - \delta\varphi_j. \quad (72)$$

Substituting this equation into equation (71), one obtains the relation:

$$\begin{aligned} S_1 &= \sum_i \sum_j I_{ij} (\delta\varphi_i - \delta\varphi_j) \\ &= \sum_i \delta\varphi_i \left(\sum_j I_{ij} \right) - \sum_j \delta\varphi_j \left(\sum_i I_{ij} \right). \end{aligned} \quad (73)$$

The sums in the brackets are equal to zero, due to the Kirchhoff's law, equation (65). Therefore $S_1 = 0$ and in the right-hand side of equation (70) only the second sum survives:

$$\delta\mathbb{P} = \sum_{(i,j)} U_{ij}^2 \delta G_{ij}. \quad (74)$$

The latter equation can be written equivalently as

$$\delta\mathbb{P} = \sum_{(i,j)} P_{ij} \frac{\delta G_{ij}}{G_{ij}} \equiv \sum_{(i,j)} P_{ij} \delta(\ln G_{ij}). \quad (75)$$

Evaluating $\delta\mathbb{P}$ from equation (68),

$$\delta\mathbb{P} = U^2 \delta G = U^2 G \frac{\delta G}{G} \equiv \mathbb{P} \delta(\ln G), \quad (76)$$

and comparing equation (75) with equation (76), we obtain

$$\delta(\ln G) = \mathbb{P}^{-1} \sum_{(i,j)} P_{ij} \delta(\ln G_{ij}). \quad (77)$$

Equation (77) makes it possible to evaluate the response of the network's conductance to variations G_{ij} of individual resistors. We will use this result for calculating the activation energy of hopping mobility and for calculating the change of the mobility when a small part of the DOS is cut out.

6.2. Activation energy of hopping conductivity and the transport energy

Let us consider mobility μ of some hopping systems as a function of temperature T . Electron concentration is assumed to be constant. One can define the activation energy ε_a as

$$\varepsilon_a = -\frac{d(\ln \mu)}{d(1/kT)}, \quad (78)$$

i.e. as a slope of the temperature dependence of mobility in the Arrhenius plot. Below we denote $1/kT$ as β .

Taking a sufficiently large sample of the conducting medium, one can assume that the conductance G of the sample is proportional to μ , as a function of temperature. Therefore

$$\varepsilon_a = -\frac{d(\ln G)}{d\beta}, \quad (79)$$

and, according to equation (77),

$$\varepsilon_a = -\mathbb{P}^{-1} \sum_{(i,j)} P_{ij} \frac{d(\ln G_{ij})}{d\beta}, \quad (80)$$

where \mathbb{P} is the sum of all P_{ij} as defined by equation (67).

Assuming Miller–Abrahams hopping rates given by equation (8), one can evaluate the conductance G_{ij} corresponding to the transition between sites i and j as

$$G_{ij} = \frac{e^2}{kT} \Gamma_{ij}^0 \exp\left(\frac{\varepsilon_F - \max(\varepsilon_i, \varepsilon_j)}{kT}\right), \quad (81)$$

where Γ_{ij}^0 is a temperature-independent prefactor that depends on the distance between the sites. Equation (81) is valid only when both ε_i and ε_j lie far above the Fermi level. This condition is fulfilled for all *decisive* transitions, for which P_{ij} is non-vanishing. We therefore will use equation (81) for *all* transitions.

Taking the derivative of equation (81), one obtains

$$\frac{d(\ln G_{ij})}{d\beta} = kT + \beta \frac{d\varepsilon_F}{d\beta} + \varepsilon_F - \max(\varepsilon_i, \varepsilon_j). \quad (82)$$

Substituting this equation into equation (80) provides the activation energy in the form:

$$\varepsilon_a = \varepsilon_2 - \varepsilon_1 - kT, \quad (83)$$

where

$$\varepsilon_1 = \beta \frac{d\varepsilon_F}{d\beta} + \varepsilon_F, \quad (84)$$

$$\varepsilon_2 = \frac{\sum_{(i,j)} P_{ij} \max(\varepsilon_i, \varepsilon_j)}{\sum_{(i,j)} P_{ij}}. \quad (85)$$

Note that ε_2 does not depend on the carrier concentration n . Indeed, the only concentration-dependent factor in equation (81) is $\exp(\varepsilon_F/kT)$, the same for all conductances G_{ij} . Therefore all ratios between conductances remain unchanged

with varying n and consequently the same is true for the ratios between powers P_{ij} contributing to equation (85).

In the case of a slowly varying DOS, such as the exponential DOS with a characteristic energy scale $\varepsilon_0 \gg kT$, the Fermi energy is almost temperature-independent. Hence, one can neglect the first term of the r.h.s. in equation (84) and get $\varepsilon_1 \approx \varepsilon_F$. According to equation (83) the activation energy ε_a is approximately equal to the distance from the Fermi level to the concentration-independent energy level ε_2 . This result resembles the schematic picture shown in figure 4(a) for the exponential DOS. In this picture, long-range transport can be understood as activation of carriers from the Fermi level to the transport energy ε_t . Thus, it is reasonable to identify the transport energy with the quantity ε_2 .

The case of a Gaussian DOS given by equation (3) is somewhat more complicated. Let us calculate ε_1 for this case. The temperature dependence of ε_F is sensitive to its relative position with regards to the equilibration energy ε_∞ determined by equation (18). When $\varepsilon_F > \varepsilon_\infty$, the Fermi level is almost independent of temperature [96]. Therefore $\varepsilon_1 \approx \varepsilon_F$ in this case. In the opposite case, $\varepsilon_F < \varepsilon_\infty$, the position of the Fermi level can be approximated by equation (52). Taking the derivative, one obtains

$$\beta \frac{d\varepsilon_F}{d\beta} \simeq -\frac{\sigma^2 \beta}{2} - \frac{1}{\beta} \ln \frac{n}{N}, \quad (86)$$

which together with equation (52) leads to the result:

$$\varepsilon_1 \simeq -\sigma^2 \beta = \varepsilon_\infty. \quad (87)$$

Thus, the quantity ε_1 for Gaussian DOS is found to be

$$\varepsilon_1 \simeq \begin{cases} \varepsilon_F, & \text{if } \varepsilon_F > \varepsilon_\infty, \\ \varepsilon_\infty, & \text{if } \varepsilon_F < \varepsilon_\infty. \end{cases} \quad (88)$$

This result shows that, in the Gaussian DOS, the quantity ε_2 determined by equation (85) plays the role of the TE. At high carrier concentrations ($\varepsilon_F > \varepsilon_\infty$), the activation energy $\varepsilon_a \approx \varepsilon_2 - \varepsilon_1$ corresponds to the transitions from the Fermi level to ε_2 , as in the case of the exponential DOS discussed above. At low carrier concentrations ($\varepsilon_F < \varepsilon_\infty$), the equilibration energy ε_∞ appears as a starting point for carrier activation instead of the Fermi level, in full accordance with the schematic picture shown in figure 4(b).

We have seen that, for both exponential DOS and Gaussian DOS, the quantity ε_2 acts as the target energy of carrier activation, i.e., as the TE. Thus, we *define* the TE ε_t as being equal to ε_2 :

$$\varepsilon_t \equiv \varepsilon_2. \quad (89)$$

According to this definition, equation (85) expresses the TE through the values of dissipated powers P_{ij} , which can be found by computer simulations.

Finally, let us offer a more convenient representation for the TE $\varepsilon_t \equiv \varepsilon_2$ defined by equation (85). Let $H(\varepsilon)$ be the sum of P_{ij} over such pairs (i, j) that $\max(\varepsilon_i, \varepsilon_j) < \varepsilon$.

$$H(\varepsilon) = \sum_{\substack{(i,j) \\ \varepsilon_i < \varepsilon \\ \varepsilon_j < \varepsilon}} P_{ij}. \quad (90)$$

Obviously, $H(\varepsilon)$ is a monotonously increasing function with limits

$$H(-\infty) = 0, \quad H(+\infty) = \sum_{(i,j)} P_{ij} \equiv \mathbb{P}. \quad (91)$$

If the sample is sufficiently large, $H(\varepsilon)$ can be considered as a smooth function and it is possible to define the following function $h(\varepsilon)$:

$$h(\varepsilon) = \mathbb{P}^{-1} \frac{dH(\varepsilon)}{d\varepsilon}. \quad (92)$$

By definition, $h(\varepsilon)$ is normalized:

$$\int_{-\infty}^{+\infty} h(\varepsilon) d\varepsilon = 1. \quad (93)$$

One can consider $h(\varepsilon)$ as the site distribution of the generated Joule heat.

The energy ε_t can be expressed via the function $h(\varepsilon)$. To show this, consider the contribution into the sum

$$\sum_{(i,j)} P_{ij} \max(\varepsilon_i, \varepsilon_j) \quad (94)$$

of such pairs (i, j) that $\max(\varepsilon_i, \varepsilon_j) \in [\varepsilon, \varepsilon + d\varepsilon]$. This contribution is equal to

$$\varepsilon [H(\varepsilon + d\varepsilon) - H(\varepsilon)] = \varepsilon \frac{dH(\varepsilon)}{d\varepsilon} d\varepsilon = \varepsilon \mathbb{P} h(\varepsilon) d\varepsilon. \quad (95)$$

Consequently, the whole sum equation (94) can be obtained by integration of equation (95):

$$\sum_{(i,j)} P_{ij} \max(\varepsilon_i, \varepsilon_j) = \int_{-\infty}^{+\infty} \varepsilon \mathbb{P} h(\varepsilon) d\varepsilon. \quad (96)$$

Dividing both parts of the latter equation by \mathbb{P} , one obtains, according to equations (85) and (89), that

$$\varepsilon_t = \int_{-\infty}^{+\infty} \varepsilon h(\varepsilon) d\varepsilon. \quad (97)$$

It means that the TE ε_t is equal to the center of mass of the heat distribution curve $h(\varepsilon)$. This is the central result of this section. It provides an accurate and easy-to-understand meaning of the TE and gives a method of evaluation ε_t from computer simulation data.

An example of heat distributions $h(\varepsilon)$ at different temperatures in the GDM is shown in figure 13. These curves were calculated numerically by the following procedure. The dissipated powers P_{ij} were obtained by numerical solution of a system of Kirchhoff's equations (see the first paragraph of section 6.1) in a cube containing $30 \times 30 \times 30$ sites with periodic boundary conditions.⁴ Conductances G_{ij} were taken in the form of equation (81) for all pairs (i, j) , assuming infinitely small carrier concentration. Then, the function $h(\varepsilon)$ was obtained from the values of P_{ij} and averaged over 50 realizations.

The curves $h(\varepsilon)$ indicate the energy ranges, at which the sites responsible for long-range transport are located.

⁴ For $kT/\sigma = 0.2$, a $60 \times 60 \times 60$ cube was used.

Sites with energies *above* this region do not participate in conductivity at all. On the other hand, some sites *below* this region are parts of current-carrying paths, but their resistances are too low to contribute to the whole network's resistance. (See [74, 75] for a spatial picture of the current paths simulated for the lattice model.) In this sense, the exact values of conductances G_{ij} for connections between such sites are not important. This justifies the argumentation based on using the 'non-degenerate' expression (81) for all pairs (i, j) even when some sites lie below the Fermi level, as long as the Fermi level is below the range of non-vanishing $h(\varepsilon)$. Under these circumstances, the function $h(\varepsilon)$ does not depend on the carrier concentration. (The reasoning above, as to why the transport energy ε_t is concentration-independent, can be applied to the function $h(\varepsilon)$ as well.)

Figure 13 clearly demonstrates the VRH nature of conduction in the GDM. The very essence of VRH is the temperature dependence of the optimal hops. With decreasing temperature, a carrier is forced to choose upward hops to sites lower in energy but more distant in space. Consequently, the smaller the temperature is, the lower is the energy range of sites decisive in the long-range transport. This tendency is seen in figure 13: the curve $h(\varepsilon)$ and, concomitantly, the TE, shifts downwards with decreasing temperature.

Let us briefly summarize the main results from this section:

1. The heat distribution function $h(\varepsilon)$ indicates the range of energies of the most important sites for the long-range transport. The TE ε_t is located in the middle of this energy range and is related to the function $h(\varepsilon)$ by equation (97).
2. The activation energy ε_a of hopping conduction is equal to $\varepsilon_t - \varepsilon_1 - kT$, where the quantity ε_1 is defined by equation (84). This can be interpreted as follows: in order to participate in the long-range conduction, carriers should be thermally activated from the level ε_1 to the transport level ε_t (the additional term $-kT$ is related to a pre-exponential factor). For exponential DOS, $\varepsilon_1 \approx \varepsilon_F$. The same is true for Gaussian DOS at high enough carrier concentrations, $n > n_c$. If carrier concentration is low ($n < n_c$) in the case of Gaussian DOS, ε_1 approaches the equilibration energy $\varepsilon_\infty = -\sigma^2/kT$.
3. The transport energy ε_t can be easily calculated on the basis of computer simulations of hopping transport, either from dissipated powers P_{ij} by equation (85), or from the heat distribution $h(\varepsilon)$ by equation (97). Both these formulas are exact.
4. In the VRH regime, the heat distribution $h(\varepsilon)$ and the TE ε_t move downwards with decreasing temperature. This reflects the interplay between the spatial and energetical terms in the typical rate of an upward hop, given by equation (58) and is the essence of the VRH.
5. The concept of the transport energy is applicable when the Fermi level ε_F lies well below the curve $h(\varepsilon)$ (i.e. when $h(\varepsilon_F)$ is negligible). In this regime, the function $h(\varepsilon)$ and concomitantly the transport energy ε_t do not depend on the carrier concentration.

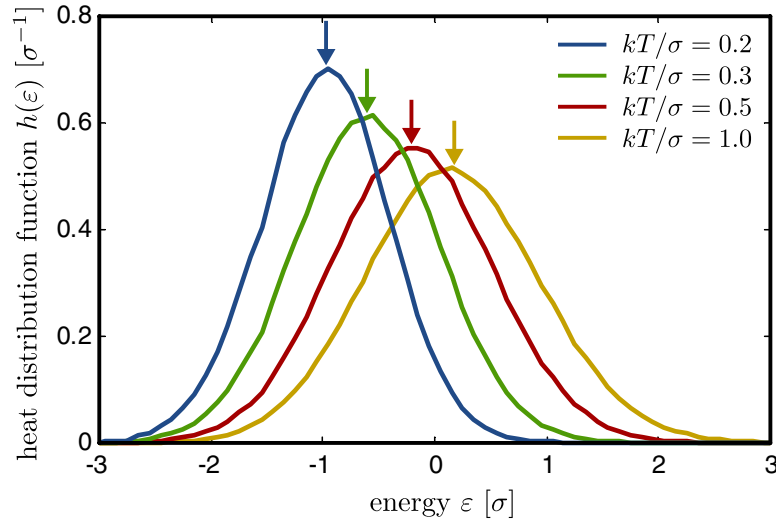


Figure 13. Heat distribution functions $h(\varepsilon)$ at four different temperatures in the system with Gaussian DOS and randomly placed sites (GDM). Arrows indicate positions of the transport energy, calculated by equation (97), at corresponding temperatures. Localization length $\alpha = 0.3 N^{-1/3}$.

6.3. Distribution of dissipated heat over hopping distances

In the full analogy with the distribution of dissipated heat over energies, $h(\varepsilon)$, one can introduce the heat distribution function over hopping distances, $h_r(r)$:

$$h_r(r) = \mathbb{P}^{-1} \frac{dH_r(r)}{dr}, \quad (98)$$

where

$$H_r(r) = \sum_{\substack{(i,j) \\ r_{ij} < r}} P_{ij}. \quad (99)$$

Let us also introduce the notation \bar{r} for the ‘mean hopping distance’, where the mean value is taken using the dissipated powers P_{ij} as weights:

$$\bar{r} = \frac{\sum_{(i,j)} P_{ij} r_{ij}}{\sum_{(i,j)} P_{ij}}. \quad (100)$$

The relation between the function $h_r(r)$ and the quantity \bar{r} is analogous to the relation between $h(\varepsilon)$ and ε_t :

$$\bar{r} = \int_{-\infty}^{+\infty} r h_r(r) dr, \quad (101)$$

i.e. \bar{r} is the center of mass of the distribution $h_r(r)$.

In addition, the physical meaning of $h_r(r)$ and \bar{r} are analogous to that of $h(\varepsilon)$ and ε_t . The value of \bar{r} reflects the typical length of hops decisive for conductivity and the curve $h_r(r)$ shows the distribution of such hops. The distributions $h_r(r)$ are given in figure 14 for the same model and parameters used in the previous section for figure 13. One can see that the distributions are restricted from above and from below. With decreasing temperature, the curve $h_r(r)$ shifts towards larger hopping lengths. This is again a direct evidence of the variable-range hopping in the GDM.

Just as the TE determines the conductivity response to a small change of temperature (via the activation energy), the ‘mean hopping distance’ \bar{r} determines the response to small changes of the localization length α and of the site concentration N . To see this, recall that each elementary conductance G_{ij} is proportional to $\exp(-2r_{ij}/\alpha)$ and, consequently,

$$\frac{\partial(\ln G_{ij})}{\partial(\alpha^{-1})} = -2r_{ij}. \quad (102)$$

From equations (77) and (102) one can express the response of the logarithm of the sample’s conductance $\ln G$ to small variation of α^{-1} :

$$\frac{\partial(\ln G)}{\partial(\alpha^{-1})} = \mathbb{P}^{-1} \sum_{(i,j)} P_{ij} (-2r_{ij}) = -2\bar{r}. \quad (103)$$

Note by comparison of equations (102) and (103) that the whole sample reacts to small changes of α as if all hops had the length \bar{r} .

It is hardly possible to control α in a real experiment. More experimentally relevant is the system’s response to small changes of the site concentration N . These two kinds of responses (to α and to N) are related to each other due to the fact that α and N can appear in the conductivity σ_{dc} not independently, but only in the combination $N\alpha^3$ (apart from the factor $N^{1/3}$ that is needed by dimensionality considerations):

$$\sigma_{dc}(N, \alpha) = N^{1/3} \chi(N\alpha^3), \quad (104)$$

where χ is some unknown function. Taking logarithmic derivatives of σ_{dc} ,

$$-2\bar{r} = \frac{\partial(\ln \sigma_{dc})}{\partial(\alpha^{-1})} = -3N\alpha^4 \frac{\chi'}{\chi}, \quad (105)$$

$$\frac{\partial(\ln \sigma_{dc})}{\partial(\ln N)} = \frac{1}{3} + N\alpha^3 \frac{\chi'}{\chi}, \quad (106)$$

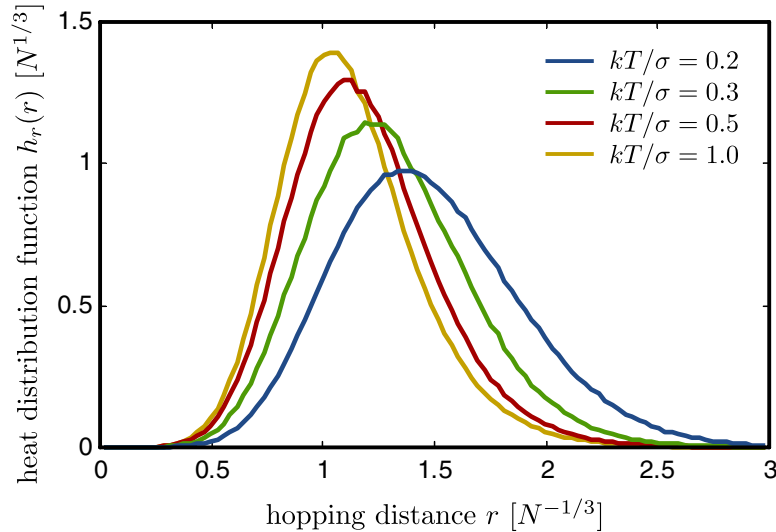


Figure 14. Heat distributions over hopping distances, $h_r(r)$, at four different temperatures in the system with Gaussian DOS and randomly placed sites (GDM). Localization length $\alpha = 0.3 N^{-1/3}$.

and excluding the function χ from equations (105) and (106), one can obtain the response of σ_{dc} to small variations of the site concentration N :

$$\frac{\partial(\ln \sigma_{dc})}{\partial(\ln N)} = \frac{1}{3} + \frac{2}{3} \frac{\bar{r}}{\alpha}. \quad (107)$$

(Note that we assumed in equations (104)–(107) that the fraction of occupied sites n/N remains constant during variation of N .)

Let us test equations (103) and (107) on the simplest case of the NNH with isoenergetic sites, as discussed in section 4.1. Applying either equation (103) or equation (107) to the solution of the NNH problem, equation (28), one can find the value of \bar{r} ,

$$\bar{r} = \frac{\gamma}{2} N^{-1/3} + \frac{\nu}{2} \alpha \equiv r_c + \frac{\nu}{2} \alpha, \quad (108)$$

where r_c is the percolation threshold determined by equation (24). In the limit $N\alpha^3 \rightarrow 0$ (strong percolation) \bar{r} tends to r_c , supporting the interpretation of \bar{r} as of the ‘length of the most important hops’.

It is also possible to study not only one-dimensional distributions of the dissipated heat, $h(\varepsilon)$ and $h_r(r)$, but also its two-dimensional distribution over the energy ε and the hopping distance r . An example of such distribution in the GDM is shown in figure 15. One can see that the major part of the heat is generated by hops placed in the (r, ε) -plane near the green line defined by the equation

$$\frac{\varepsilon}{kT} + \frac{2r}{\alpha} = \text{const} \equiv \frac{\varepsilon_G^*}{kT}. \quad (109)$$

Here ε_G^* has the meaning of the ‘effective transport energy’, which is discussed in sections 4.4 and 5. Figure 15 clearly demonstrates the difference between the ‘real’ transport energy ε_t and the ‘effective’ one, ε_G^* . Namely, sites with energies near ε_t do participate in conductivity, unlike sites with energies close to ε_G^* . The quantity ε_G^* is simply a measure of hopping difficulty including both energetical and spatial barriers.

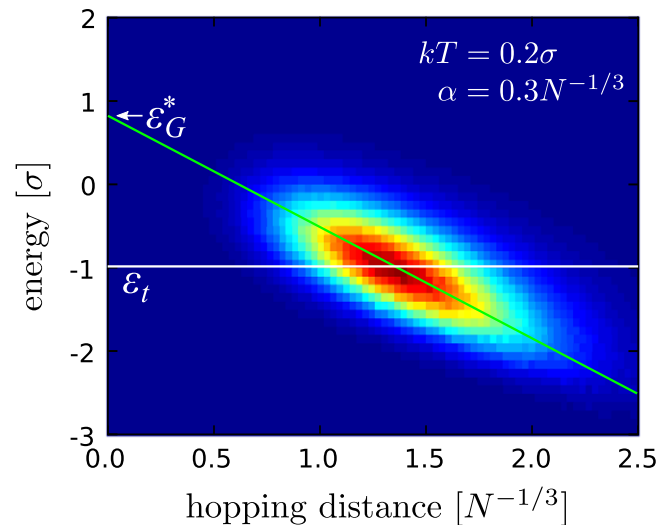


Figure 15. Distribution of the dissipated heat over hopping distances (horizontal axis) and site energies (vertical axis) in the GDM: the maximal dissipation is colored red, zero dissipation is colored blue. The white horizontal line indicates the transport energy ε_t . The green inclined line connects equally hard hops: $\varepsilon/kT + 2r/\alpha = \text{const}$. The position of the ‘effective transport energy’ ε_G^* , discussed in sections 4.4 and 5, is also shown.

6.4. Effect of cutting out small part of DOS

Having found the precise way to determine the TE via equation (97), let us check the validity of the procedure based on the method of cutting out parts of the DOS used in section 5 for the VRH. Let us calculate the change δG of the conductance G of a sample due to cutting out sites within the energy range $[\varepsilon_{\text{cut}}, \varepsilon_{\text{cut}} + w]$, while carrier concentration remains unchanged.⁵ The width w of the cut range is considered small as compared to kT . Therefore the initial DOS $g(\varepsilon)$ turns into

⁵ Unlike section 5, where ε_{cut} denotes the *upper* edge of the cut-out energy band, in this subsection we use the symbol ε_{cut} for the *lower* edge of the band. This small correction is motivated by our effort to keep the formulas as short as possible.

the following DOS $\tilde{g}(\varepsilon)$:

$$\tilde{g}(\varepsilon) = \begin{cases} 0, & \text{if } \varepsilon \in [\varepsilon_{\text{cut}}, \varepsilon_{\text{cut}} + w], \\ g(\varepsilon), & \text{otherwise,} \end{cases} \quad (110)$$

as illustrated in figure 11. Assuming that changes of all conductances caused by the DOS modification are small, one can calculate δG using equation (77). The small change of local conductances can be achieved by the following change of site energies ε_i :

$$\varepsilon_i \rightarrow \varepsilon_i + \Delta(\varepsilon_i), \quad (111)$$

where

$$\Delta(\varepsilon) = \begin{cases} 0, & \text{if } \varepsilon < \varepsilon_{\text{cut}}, \\ w g(\varepsilon_{\text{cut}})/g(\varepsilon), & \text{if } \varepsilon \geq \varepsilon_{\text{cut}}. \end{cases} \quad (112)$$

The modification of site energies given by equation (111) converts the DOS $g(\varepsilon)$ into $\tilde{g}(\varepsilon)$, while the change of all site energies is small (except very high energies that do not contribute to the charge transport). In order to keep the fixed carrier concentration n , the Fermi level ε_F must be changed as well.

Relative variations $\delta(\ln G_{ij})$ of the local conductances G_{ij} can then be found from equation (81):

$$\delta(\ln G_{ij}) = \frac{\delta\varepsilon_F}{kT} - \frac{\Delta(\max(\varepsilon_i, \varepsilon_j))}{kT}, \quad (113)$$

where $\delta\varepsilon_F$ is the change of the Fermi level. Substitution of equation (113) into equation (77) gives the relative change $\delta(\ln G)$ of the sample's conductance G :

$$\delta(\ln G) = \frac{\delta\varepsilon_F}{kT} - \frac{1}{\mathbb{P}kT} \sum_{(i,j)} P_{ij} \Delta(\max(\varepsilon_i, \varepsilon_j)). \quad (114)$$

In equation (114) one can apply the same reduction of the summation $\sum_{(i,j)} P_{ij} \dots$ to an integration $\int d\varepsilon h(\varepsilon) \dots$ that led from equation (85) to equation (97). The only difference is that $\Delta(\max(\varepsilon_i, \varepsilon_j))$ is contributing instead of $\max(\varepsilon_i, \varepsilon_j)$. The result is

$$\begin{aligned} \delta(\ln G) &= \frac{\delta\varepsilon_F}{kT} - \frac{1}{kT} \int_{-\infty}^{+\infty} h(\varepsilon) \Delta(\varepsilon) d\varepsilon \\ &= \frac{\delta\varepsilon_F}{kT} - \frac{w}{kT} \int_{\varepsilon_{\text{cut}}}^{+\infty} h(\varepsilon) \frac{g(\varepsilon_{\text{cut}})}{g(\varepsilon)} d\varepsilon. \end{aligned} \quad (115)$$

Finally, let us find $\delta\varepsilon_F$ from the following condition of constant carrier concentration n :

$$\begin{aligned} n &= \int_{-\infty}^{\infty} g(\varepsilon) f(\varepsilon, \varepsilon_F) d\varepsilon \\ &= \int_{-\infty}^{\infty} \tilde{g}(\varepsilon) f(\varepsilon, \varepsilon_F + \delta\varepsilon_F) d\varepsilon, \end{aligned} \quad (116)$$

where $f(\varepsilon, \varepsilon_F)$ is the Fermi function. The right-hand side can be rewritten (using smallness of $\delta\varepsilon_F$ and w) as follows:

$$n = n + \frac{dn}{d\varepsilon_F} \delta\varepsilon_F - g(\varepsilon_{\text{cut}}) f(\varepsilon_{\text{cut}}, \varepsilon_F) w, \quad (117)$$

from where one can find

$$\delta\varepsilon_F = w \frac{g(\varepsilon_{\text{cut}}) f(\varepsilon_{\text{cut}}, \varepsilon_F)}{dn/d\varepsilon_F}. \quad (118)$$

Substitution of $\delta\varepsilon_F$ given by equation (118) into equation (115) provides the final result:

$$\begin{aligned} \frac{\delta G}{G} &= \frac{w}{kT} \frac{g(\varepsilon_{\text{cut}}) f(\varepsilon_{\text{cut}}, \varepsilon_F)}{dn/d\varepsilon_F} \\ &\quad - \frac{w}{kT} \int_{\varepsilon_{\text{cut}}}^{\infty} h(\varepsilon) \frac{g(\varepsilon_{\text{cut}})}{g(\varepsilon)} d\varepsilon. \end{aligned} \quad (119)$$

The first (positive) term is responsible for moving the Fermi energy upward due to cutting off part of the DOS, while the second (negative) one reflects a moving upward of the TE.

Figure 16 provides an illustration to equation (119). The upper plot reproduces the heat distribution function $h(\varepsilon)$ taken from figure 13 at $kT = 0.3\sigma$. The lower plot shows the corresponding dependence $\delta G(\varepsilon_{\text{cut}})$. It is clearly visible that figure 16 reproduces all features of figure 12, where the effect of the cut-off was simulated straightforwardly: The region of positive δG near the equilibration energy ε_{∞} is described by the first term in equation (119), while the decrease of δG at higher energies reflects the impact of cutting out sites around the transport path (second term in equation (119)).

The quantity δG takes negative values in figure 16 only within the range of non-vanishing $h(\varepsilon)$, i.e. near the TE ε_t . This can be easily understood on the basis of equation (119). When ε_{cut} is too high, the function $h(\varepsilon)$ vanishes at $\varepsilon > \varepsilon_{\text{cut}}$ and so does the integral in equation (119). If ε_{cut} is too low, this integral is proportional to $g(\varepsilon_{\text{cut}})$, therefore strongly decaying with lowering ε_{cut} .

With the above results one can conclude that the procedure based on cutting out parts of the DOS used in section 5 is valid. The TE $\varepsilon_t^{\text{cut}}$ obtained by this procedure (the minimum position of the curve $\delta G(\varepsilon_{\text{cut}})$) is located in the region of energies decisive for the long-range transport. The same is true for the TE ε_t derived from the heat distribution as explained in section 6.2. However, one can see in figures 12 and 16 that $\varepsilon_t^{\text{cut}}$ appears slightly lower than TEs determined by other methods. The reason for that lies in the fact that cutting-out sites *below* the transport energy causes a larger effect in the conductivity than cutting-out sites *above* the TE.

One can conclude that the energy distribution of the dissipated heat, $h(\varepsilon)$, provides enough information to predict the response of conductivity on small changes of the DOS. Together with the observations of sections 6.2 and 6.3, it makes the heat method presented here a powerful tool for analyzing the hopping conductivity in organic materials.

The heat method developed in this section was illustrated in the example of GDM. It should be noted, however, that the method can be applied to other models as well, including the exponential DOS model and the Correlated Disorder Model (CDM). It is especially notable that in the case of CDM, where existence of a transport energy was in doubt, the heat method also provides a meaningful definition of the transport energy.

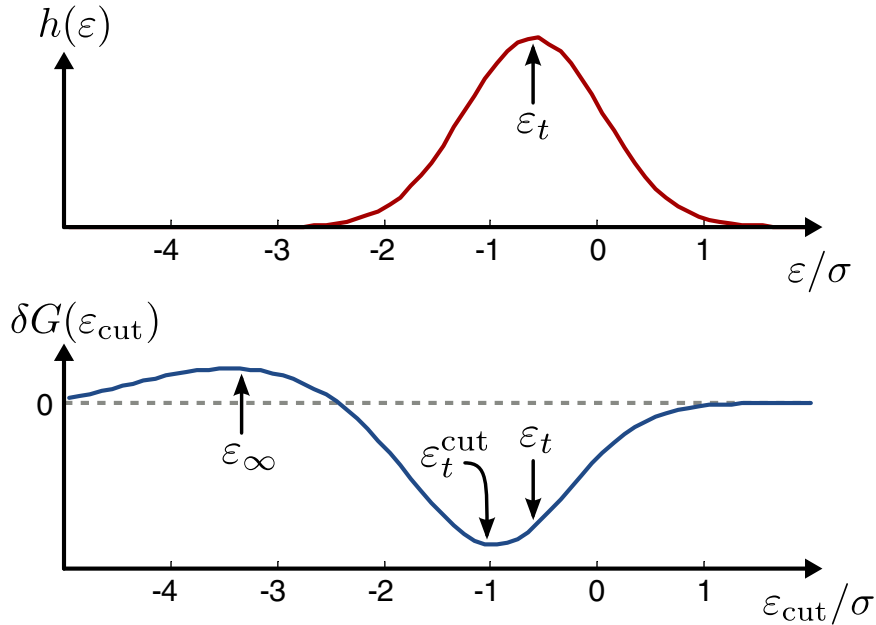


Figure 16. Heat distribution function $h(\varepsilon)$ (upper plot) and change in conductivity $\delta G(\varepsilon_{\text{cut}})$ when a small part of the DOS near the energy ε_{cut} is cut out (lower plot) for GDM. Parameters: $\alpha = 0.3 N^{-1/3}$, $kT = 0.3\sigma$, $\varepsilon_F = -5\sigma$. Indicated energies: the equilibration energy ε_∞ , the transport energy ε_t defined from the heat distribution and the transport energy $\varepsilon_t^{\text{cut}}$ defined by the cutting method introduced in section 5.

7. WoT: On the effective medium approximation

Effective medium approximation (EMA) belongs to the theoretical tools often used to study charge transport in disordered systems [120–122] including ODSs [26, 123]. The EMA is based on the averaging of various characteristics of the inhomogeneous media [73]. Starting from the method of a random resistor network considered in section 4, the EMA leads to the following self-consistency equation for the effective conductance G between hopping sites,

$$\left\langle \frac{G_{ij} - G}{G_{ij} + \chi G} \right\rangle = 0, \quad (120)$$

where G_{ij} is the random quantity describing the conductance between sites i and j in the random resistor network. The symbol $\langle \rangle$ denotes the configurational averaging and $\chi = d - 1$, where d is the spatial dimension of the considered problem [120, 122].

The EMA has been applied to study both the NNH transport regime [26, 121] and the VRH regime [122, 124]. Remarkably, many results obtained in the framework of the EMA [122, 124] differ essentially from those obtained in the framework of the percolation theory [73, 94]. For instance, at low temperatures, when hopping conduction occurs in the narrow energy range in close proximity to the Fermi level, the temperature dependence of the hopping conductivity in the VRH regime is predicted in the framework of the EMA for $d = 3$ in the form [122]

$$\sigma_{\text{dc}} = \tilde{\sigma}_{\text{dc}}^0 \exp[-(\tilde{T}_0/T)^{2/5}], \quad (121)$$

where \tilde{T}_0 is the characteristic temperature and the prefactor $\tilde{\sigma}_{\text{dc}}^0$ depends on temperature weakly.

Apparently, this result conflicts with the prominent Mott law [88] given by equation (38). Overhof and Thomas [94] analyzed the disagreement between equation (121) and equation (38) and came to the conclusion that equation (121) provided by the EMA is not sufficiently accurate, whereas equation (38) can be viewed as valid. A similar result with respect to the accuracy of the EMA can be found in the monograph by Shklovskii and Efros [73], who concluded that ‘*the effective medium theory gives accurate results only in the case of a weak relative inhomogeneity. This approach, by its very essence, cannot lay claim to good results for a strongly (exponentially) inhomogeneous medium.*’ For weakly inhomogeneous systems, the EMA might be applicable, but such systems are not within the scope of the current review article.

8. Summary

Though claiming in the title of this review that the paper is related to theoretical treatment of charge transport in organic disordered semiconductors (ODSs), we have not focused strongly on specific details of ODSs. Instead, the main content of the article is devoted to general theoretical tools suitable to describe hopping transport in strongly inhomogeneous media. These general tools are applicable to the ODSs since it is widely concluded in the community that the transport mechanism in these materials is hopping transport [13–24].

What is, however, specific to the state of research related to charge transport in ODSs is the unawareness of large parts of the community with respect to the general theoretical tools suitable to successfully describe hopping transport. Therefore, much emphasis in the research on ODSs has so far been put on the phenomenological fitting of results obtained in numerical calculations, by equations containing numerous

adjustable parameters. The most popular examples of such phenomenological fittings are provided by equations (5)–(7), which are shown in section 2 as hardly acceptable. Furthermore, it is shown in section 3 that forcing charge carriers to perform only the nearest-neighbour transitions on a regular lattice grid, performed in several recent theoretical studies, can hardly bring meaningful results if the thermal energy kT is smaller than the energy scale of disorder, as is typical for ODSs at room temperature. The disproportion in the theoretical research on ODSs between the world of simulations (WoS) and the world of theory (WoT) is still remarkable.

In sections 4 and 5 we highlighted the percolation theory and the concept of transport energy (TE) as suitable tools to describe the variable-range hopping transport in strongly inhomogeneous disordered systems, including the ODSs. These well-approved theoretical tools, developed initially for applications in the field of inorganic materials, are perfectly suitable to describe charge transport in ODSs. Among other results, it is shown that transport features are sensitive to the energy spectrum of the system. For instance, in systems with the density of states steeper than the exponential function, carrier mobility μ does not depend on the concentration of carriers n at low n values, while in systems with the DOS described by an exponential or by a weaker energy-dependent function, μ , on the contrary, depends on n at all n values.

In section 6 a novel analytical approach based on calculations of the heat power production in the random resistor network is described as an accurate tool to study hopping transport. This accurate theoretical tool confirms the validity and accuracy of the TE concept.

Among the not yet clarified issues, one could highlight the question as to whether the GDM or the CDM (correlated disorder model) is more realistic for ODSs and the question on the role of polaron effects for charge transport in ODSs. Furthermore, one should go beyond the simplest set of phenomenological assumptions, which is the basis for the GDM and CDM. Some existing theoretical attempts in this direction were however beyond the scope of our review.

Acknowledgments

Financial support by the Deutsche Forschungsgemeinschaft (Grants No. BA 1298/9-1 and No. GRK 1782) is gratefully acknowledged.

References

- [1] Tang C W and Van Slyke S A 1987 *Appl. Phys. Lett.* **51** 913
- [2] Burroughes J H, Bradley D D C, Brown A R, Marks R N, Mackay K, Friend R H, Burns P L and Holmes A B 1990 *Nature* **347** 539
- [3] Brown A R, Jarrett C P, de Leeuw D M and Matters M 1997 *Synth. Met.* **88** 37
- [4] Yu G, Gao J, Hummelen J C, Wudl F and Heeger A J 1995 *Science* **270** 1789
- [5] Abkowitz M 1992 *Phil. Mag.* B **65** 817
- [6] Kryukov A Y, Saidov A C and Vannikov A V 1992 *Thin Solid Films* **209** 84
- [7] Gill W 1972 *J. Appl. Phys.* **43** 5033
- [8] Schein L A, Peled A and Glatz D 1989 *J. Appl. Phys.* **66** 686
- [9] Bässler H 1993 *Phys. Status Solidi B* **175** 15
- [10] Borsenberger P M and Shi J 1995 *Phys. Status Solidi B* **191** 461
- [11] Borsenberger P M, Gruenbaum W T and Magin E H 1996 *Physica B* **228** 226
- [12] Bässler H 1981 *Phys. Status Solidi B* **107** 9
- [13] Borsenberger P M, Magin E H, van der Auweraer M and de Schryver F C 1993 *Phys. Status Solidi A* **140** 9
- [14] van der Auweraer M, de Schryver F C, Borsenberger P M and Bässler H 1994 *Adv. Mater.* **6** 199
- [15] Pope M and Swenberg C E 1999 *Electronic Processes in Organic Crystals and Polymers* (Oxford: Oxford University Press)
- [16] Hadziioannou G and van Hutten P F (ed) 2000 *Semiconducting Polymers* (New York: Wiley)
- [17] Brabec C, Dyakonov V, Parisi J and Sariciftci N (ed) 2003 *Organic Photovoltaics: Concepts and Realization* (Berlin: Springer)
- [18] Brütting W (ed) 2005 *Physics of Organic Semiconductors* (New York: Wiley)
- [19] Baranovski S (ed) 2006 *Charge Transport in Disordered Solids with Applications in Electronics* (Chichester: Wiley)
- [20] Schwoerer M and Wolf H C 2007 *Organic Molecular Solids* (New York: Wiley)
- [21] Sun S S and Dalton L (ed) 2008 *Organic Electronic and Optoelectronic Materials and Devices* (Boca Raton, FL: CRC Press)
- [22] Tessler N, Preezant Y, Rappaport N and Roichman Y 2009 *Adv. Mater.* **21** 2741
- [23] Meller G and Grasser T (ed) 2010 *Organic Electronics* (Berlin: Springer)
- [24] Baranovskii S D 2014 *Phys. Status Solidi B* **251** 487
- [25] Miller A and Abrahams E 1960 *Phys. Rev.* **120** 745
- [26] Fishchuk I I, Kadashchuk A, Hoffmann S T, Athanasopoulos S, Genoe J, Bässler H and Köhler A 2013 *Phys. Rev. B* **88** 125202
- [27] Marcus R A 1964 *Ann. Rev. Phys. Chem.* **15** 155
- [28] Rubel O, Baranovskii S. D, Thomas P and Yamasaki S 2004 *Phys. Rev. B* **69** 014206
- [29] Bredas J L, Beljonne D, Coropceanu V and Cornil J 2004 *Chem. Rev.* **104** 4971
- [30] Martens H C F, Blom P W M and Schoo H F M 2000 *Phys. Rev. B* **61** 7489
- [31] Arkhipov V I, Heremans P, Emelianova E V, Adriaenssens G J and Bässler H 2002 *J. Phys.: Condens. Matter* **14** 9899
- [32] Tanase C, Blom P W M, de Leeuw D M and Meijer E J 2004 *Phys. Status Solidi A* **201** 1236
- [33] Pasveer W F, Cottaar J, Tanase C, Coehoorn R, Bobbert P A, Blom P W M, de Leeuw D M and Michels M A J 2005 *Phys. Rev. Lett.* **94** 206601
- [34] Arkhipov V I, Heremans P, Emelianova E V and Bässler H 2005 *Phys. Rev. B* **71** 045214
- [35] Craciun N I, Wildeman J and Blom P W M 2008 *Phys. Rev. Lett.* **100** 056601
- [36] Germs W C, van der Holst J J M, van Mensfoort S L M, Bobbert P A and Coehoorn R 2011 *Phys. Rev. B* **84** 165210
- [37] Mendels D and Tessler N 2013 *J. Phys. Chem. C* **117** 24740
- [38] Oelerich J O, Huemmer D and Baranovskii S D 2012 *Phys. Rev. Lett.* **108** 226403
- [39] Gartstein Y N and Conwell E M 1995 *Chem. Phys. Lett.* **245** 351
- [40] Novikov S V, Dunlap D H, Kenkre V M, Parris P E and Vannikov A V 1998 *Phys. Rev. Lett.* **81** 4472
- [41] Vissenberg M C J M and Matters M 1998 *Phys. Rev. B* **57** 12964

- [42] Meijer E J, Tanase C, Blom P W M, van Veenendaal E, Huisman B H, de Leeuw D M and Klapwijk T M 2002 *Appl. Phys. Lett.* **80** 3838
- [43] Tanase C, Meijer E, Blom P and de Leeuw D 2003 *Phys. Rev. Lett.* **91** 216601
- [44] Tanase C, Meijer E, Blom P and de Leeuw D 2003 *Org. Electron.* **4** 33
- [45] Nelson J 2003 *Phys. Rev. B* **67** 155209
- [46] Tanase C, Blom P and de Leeuw D 2004 *Phys. Rev. B* **70** 193202
- [47] Salleo A, Chen T W, Völkel A R, Wu Y, Liu P, Ong B S and Street R A 2004 *Phys. Rev. B* **70** 115311
- [48] Nelson J, Choulis S and Durrant J 2004 *Thin Solid Films* **451–2** 508
- [49] Anthopoulos T, Tanase C, Setayesh S, Meijer E J, Hummelen J C, Blom P W M and de Leeuw D M 2004 *Adv. Mater.* **16** 2174
- [50] Blom P W M, Tanase C, de Leeuw D M and Coehoorn R 2005 *Appl. Phys. Lett.* **86** 092105
- [51] Sedghi N, Donaghy D, Raja M, Badriya S, Higgins S and Eccleston W 2006 *J. Non-Cryst. Solids* **352** 1641
- [52] Estrada M, Mejia I, Cerdeira A, Pallares J, Marsal L and Iiguez B 2008 *Solid-State Electron.* **52** 787
- [53] Gonzalez-Vazquez J, Anta J and Bisquert J 2009 *Phys. Chem. Chem. Phys.* **11** 10359
- [54] Tachyia M and Seki K 2010 *Phys. Rev. B* **82** 085201
- [55] Montero J and Bisquert J 2011 *J. Appl. Phys.* **110** 043705
- [56] Street R A, Song K W, Northrup J E and Cowan S 2011 *Phys. Rev. B* **83** 165207
- [57] Germs W C, Guo K, Janssen R A J and Kemerink M 2012 *Phys. Rev. Lett.* **109** 016601
- [58] Brondijk J J, Roelofs W S C, Mathijssen S G J, Shehu A, Cramer T, Biscarini F, Blom P W M and de Leeuw D M 2012 *Phys. Rev. Lett.* **109** 056601
- [59] Schubert M, Preis E, Blakesley J C, Pingel P, Scherf U and Neher D 2013 *Phys. Rev. B* **87** 024203
- [60] Borsenberger P M and Fitzgerald J J 1993 *J. Phys. Chem.* **97** 4815
- [61] Kageyama H, Ohnishi K, Nomura S and Shirota Y 1997 *Chem. Phys. Lett.* **277** 137
- [62] Laqui F, Wegner G and Bässler H 2007 *Phil. Trans. R. Soc. A* **365** 1473
- [63] Shklovskii B I 1973 *Sov. Phys. Semicond.* **6** 1964
- [64] Cleve B, Hartenstein B, Baranovskii S. D., Scheidler M, Thomas P and Bässler H 1995 *Phys. Rev. B* **51** 16705
- [65] Jansson F, Baranovskii S D, Sliužys G, Österbacka R and Thomas P 2008 *Phys. Status Solidi C* **5** 722–4
- [66] Coehoorn R and Bobbert P A 2012 *Phys. Status Solidi A* **209** 2354
- [67] Baranovskii S D, Zvyagin I P, Cordes H, Yamasaki S and Thomas P 2002 *Phys. Status Solidi B* **230** 281
- [68] Baranovskii S D, Zvyagin I P, Cordes H, Yamasaki S and Thomas P 2002 *J. Non-Cryst. Solids* **299** 416
- [69] Schmechel R 2002 *Phys. Rev. B* **66** 235206
- [70] Schmechel R 2003 *J. Appl. Phys.* **93** 4653
- [71] Shaked S, Tal S, Roichman Y, Razin A, Xiao S, Eichen Y and Tessler N 2003 *Adv. Mater.* **15** 913
- [72] Roichman Y and Tessler N 2003 *Synth. Met.* **135** 443
- [73] Shklovskii B I and Efros A L 1984 *Electronic Properties of Doped Semiconductors* (Berlin: Springer)
- [74] Cottaar J, Koster L J A, Coehoorn R and Bobbert P A 2011 *Phys. Rev. Lett.* **107** 136601
- [75] Cottaar J, Coehoorn R and Bobbert P A 2012 *Phys. Rev. B* **85** 245205
- [76] Landau L D and Lifshitz E M 1965 *Quantum Mechanics: Non-Relativistic Theory* (Oxford: Pergamon)
- [77] Ries B, Bässler H, Grünewald M and Movaghar B 1988 *Phys. Rev. B* **37** 5508
- [78] Oelerich J O, Huemmer D, Weseloh M and Baranovskii S D 2010 *Appl. Phys. Lett.* **97** 143302
- [79] Campbell I H, Smith D L, Neef C J and Ferraris J P 1999 *Appl. Phys. Lett.* **75** 841
- [80] Schulze K, Riede M, Brier E, Reinold E, Bäuerle P and Leo K 2008 *J. Appl. Phys.* **104** 074511
- [81] Alesi S, Brancolini G, Viola I, Capobianco M L, Venturini A, Camaioni N, Gigli G, Melucci M and Barbarella G 2009 *Chem. Eur. J.* **15** 1876
- [82] Ambegaokar V, Halperin B I and Langer J S 1971 *Phys. Rev. B* **4** 2612
- [83] Dalton N W, Domb C and Sykes M F 1964 *Proc. Phys. Soc.* **83** 496
- [84] Domb C and Dalton N W 1966 *Proc. Phys. Soc.* **89** 859
- [85] Lorenz C D and Ziff R M 2001 *J. Chem. Phys.* **114** 3659
- [86] Dyre J C and Schröder T B 2000 *Rev. Mod. Phys.* **72** 873
- [87] Lorenz C D and Ziff R M 1998 *Phys. Rev. E* **57** 230
- [88] Mott N F 1969 *Phil. Mag.* **19** 835
- [89] Grünewald M and Thomas P 1979 *Phys. Status Solidi B* **94** 125
- [90] Shklovskii B I and Efros A L 1971 *Sov. Phys.—JETP* **33** 468
- [91] Pollak M 1972 *J. Non-Cryst. Solids* **11** 1
- [92] Coehoorn R, Pasveer W F, Bobbert P A and Michels M A J 2005 *Phys. Rev. B* **72** 155206
- [93] Overhof H 1975 *Phys. Status Solidi B* **67** 709
- [94] Overhof H and Thomas P 1996 *Phys. Rev. B* **53** 13187
- [95] Nenashev A V, Jansson F, Oelerich J O, Huemmer D, Dvurechenskii A V, Gebhard F and Baranovskii S D 2013 *Phys. Rev. B* **87** 235204
- [96] Zvyagin I P 2008 *Phys. Status Solidi C* **5** 725
- [97] Baranovskii S D, Cordes H, Hensel F and Leising G 2000 *Phys. Rev. B* **62** 7934
- [98] Monroe D 1985 *Phys. Rev. Lett.* **54** 146
- [99] Baranovskii S D, Thomas P and Adriaenssens G J 1995 *J. Non-Cryst. Solids* **190** 283
- [100] Baranovskii S D, Faber T, Hensel F and Thomas P 1997 *J. Phys. C* **9** 2699
- [101] Noolandi J 1977 *Phys. Rev. B* **16** 4466
- [102] Schmidlin F W 1977 *Phys. Rev. B* **16** 2362
- [103] Silver M and Cohen L 1977 *Phys. Rev. B* **15** 3276
- [104] Rudenko A I and Arkhipov V I 1982 *Phil. Mag.* **B 45** 177
- [105] Arkhipov V I and Rudenko A I 1982 *Phil. Mag.* **B 45** 189
- [106] Nenashev A V, Jansson F, Baranovskii S D, Österbacka R, Dvurechenskii A V and Gebhard F 2010 *Phys. Rev. B* **81** 115204
- [107] Arkhipov V I, Emelianova E V and Bässler H 2001 *Phil. Mag.* **B 81** 985
- [108] Nikitenko V R, von Seggern H and Bässler H 2007 *J. Phys.: Condens. Matter* **19** 136210
- [109] Arkhipov V I, Heremans P and Bässler H 2003 *Appl. Phys. Lett.* **82** 4605
- [110] Martens H C F, Hulea I N, Romijn I, Brom H B, Pasveer W F and Michels M A J 2003 *Phys. Rev. B* **67** 121203
- [111] Oelerich J O, Jansson F, Nenashev A V, Gebhard F and Baranovskii S D 2014 *J. Phys.: Condens. Matter* **26** 255801
- [112] Orenstein J and Kastner M 1981 *Solid State Commun.* **40** 85
- [113] Neumann F, Genenko Y A and von Seggern H 2006 *J. Appl. Phys.* **99** 013704
- [114] Hartenstein B and Bässler H 1995 *J. Non-Cryst. Solids* **190** 112
- [115] Novikov S V and Malliaras G G 2006 *Phys. Status Solidi B* **243** 387
- [116] Arkhipov V I, Emelianova E V and Adriaenssens G J 2001 *Phys. Rev. B* **64** 125125
- [117] Yu Z G, Smith D L, Saxena A, Martin R L and Bishop A R 2000 *Phys. Rev. Lett.* **84** 721
- [118] Cottaar J and Bobbert P A 2006 *Phys. Rev. B* **74** 115204

- [119] Roichman Y and Tessler N 2002 *Appl. Phys. Lett.* **80** 1948
- [120] Kirkpatrick S 1973 *Rev. Mod. Phys.* **45** 574
- [121] Böttger H, Bryksin V V and Schulz F 1994 *Phys. Rev. B* **49** 2447
- [122] Bleibaum O, Böttger H, Bryksin V V and Schulz F 1995 *Phys. Rev. B* **51** 14020
- [123] Fishchuk I I, Arkhipov V I, Kadashchuk A, Heremans P and Bässler H 2007 *Phys. Rev. B* **76** 045210
- [124] Mott N F and Twose W 1961 *Adv. Phys.* **10** 707